

**ELECTROSPRAY ION MOBILITY – TIME OF FLIGHT
– MASS SPECTROMETRY FOR THE DETECTION OF
INORGANIC ANIONS AND PROTEINS IN AQUEOUS
MEDIA**

BY

STEVEN JOHN KLOPSCH

**A thesis submitted in partial fulfillment of
the requirements for the degree of**

MASTER OF SCIENCE

**WASHINGTON STATE UNIVERSITY
Department of Chemistry**

DECEMBER 2007

To the Faculty of Washington State University:

The members of the committee appointed to examine the thesis of STEVEN JOHN KLOPSCH find it satisfactory and recommend that it be accepted.

Chair

ACKNOWLEDGMENTS

I'd like to thank my wife Jorene Klopsch for bearing with me when I couldn't decide what to do with my life, uprooted our family and decided to go back school. Then, after changing my mind once again and coming back home, encouraged me to keep writing even though I was way over extended and my writing meant she had the burden of our home and children. Likewise I'd like to thank my father John Klopsch for riding me about finishing when part of me would just as soon forget about it. Thank you to my mother, Jean Klopsch, for always supporting me and pushing me to excel in everything I've started.

Dr. Herbert Hill – thank you for teaching me how to do science and for bearing with a student who took two years to write a thesis. I so greatly appreciate your understanding of my situation and your willingness to work through it with me – for a student who wasn't working in your lab anymore I demanded a great deal of your time and I thank you for not giving up on me. Likewise thank you to my committee members, Dr. Sue Clark and Dr. James Bruce for taking time out of your busy schedules to work with a student whom you haven't seen in two years.

Thank you to Drs. Brian Clowers, Wes Steiner and Prabha Dwivedi for their guidance and help in the lab and throughout the writing process as they guided me in the everyday realities of working in a lab and writing about it afterwards.

Finally, thank you to my Lord and Savior Jesus Christ for blessing my with family and friends who love and support me, two precious children whom I couldn't love more and the meaning and purpose found only through a life of faith.

ELECTROSPRAY ION MOBILITY – TIME OF FLIGHT – MASS SPECTROMETRY FOR THE DETECTION OF INORGANIC ANIONS AND PROTEINS IN AQUEOUS MEDIA

Abstract

by Steven John Klopsch M.S.
Washington State University
December 2007

Chair: Herbert H. Hill, Jr.

Electrospray ionization – atmospheric pressure – ion mobility – time of flight – mass spectrometry is used as a tool to investigate:

A) [Chapters 2 &3] The likelihood of using a stand alone IMS for field analysis of inorganic anionic environmental contaminants and/or biotoxins, represented in this case by small proteins of similar mass, found in aqueous media – i.e. drinking water, storm water runoff, lakes, rivers, etc... This was achieved by relating reduced mobility values to various mass identified analytes of interest as well as looking for baseline resolution of both individual anions and proteins as well as synthetic mixtures that presumably mimic what might be seen in a real world sample. In addition two actual samples, taken in Seattle, WA, are analyzed for the presence of anionic environmental contaminants of interest using the ESI-AP-IMtofMS instrument.

B) [Chapter 3] The application of protein charge state trend lines, as identified in an ESI-AP-IMtofMS experiment, to the identification of intact proteins in mixtures, as might be done in the field of proteomics, is investigated. Some success with rapid identification of proteins in a mixture, based on said trend lines, is realized.

TABLE OF CONTENTS

| | Page |
|--|------|
| ACKNOWLEDGMENTS..... | iii |
| ABSTRACT..... | iv |
| TABLE OF CONTENTS..... | v |
| LIST OF TABLES..... | viii |
| LIST OF FIGURES..... | ix |
| CHAPTER 1 | |
| I. INTRODUCTION..... | 1 |
| a) Brief History | 1 |
| b) How IMS works..... | 1 |
| c) IMS Theory..... | 3 |
| d) Ion Mobility Mass Spectrometry..... | 5 |
| II. APPLICATION OF IMtofMS ANALYSIS TO INORGANIC CONTAMINANT DETECTION..... | 6 |
| a) Why Analyze for Inorganic Contaminants?..... | 6 |
| b) Current Analytical Practices..... | 6 |
| c) ESI-IMtofMS and Inorganic Contaminant Analysis | 7 |
| III. APPLICATION OF IMtofMS TO BIOMOLECULES..... | 9 |
| a) Why Analyze Biomolecules?..... | 9 |
| b) IMS and IMMS Analysis of Individual Proteins..... | 9 |
| c) IMMS Analysis of Protein Digests and CID..... | 11 |
| d) Protein Mixtures..... | 13 |

| | |
|--|-----------|
| IV. Specific Aims..... | 15 |
| CHAPTER 2 - Determination of Inorganic Anions in Aqueous Samples by Ion Mobility | |
| Time-of-Flight Mass Spectrometry (IMtofMS) | 22 |
| I. ABSTRACT..... | 23 |
| II. INTRODUCTION..... | 24 |
| III. EXPERIMENTAL..... | 27 |
| a) Instrumentation..... | 27 |
| b) Chemicals..... | 30 |
| c) Calculations..... | 30 |
| IV. RESULTS AND DISCUSSION..... | 31 |
| V. CONCLUSIONS..... | 38 |
| VI. ACKNOWLEDGMENTS..... | 39 |
| VII. REFERENCES..... | 40 |
| CHAPTER 3 - Separation and Detection of a Protein Mixture using Ion Mobility Time-of- | |
| Flight Mass Spectrometry | 48 |
| I. ABSTRACT..... | 49 |
| II. INTRODUCTION..... | 50 |
| a) Individual Proteins..... | 50 |
| b) Protein Digests and CID Analysis..... | 52 |
| c) Protein Mixtures..... | 56 |
| III. EXPERIMENTAL..... | 57 |
| a) Chemicals, Solvents and Samples..... | 57 |
| b) Instrumentation..... | 57 |

| | |
|--|----|
| c) Calculations..... | 58 |
| IV. RESULTS AND DISCUSSION..... | 58 |
| a) Individual Proteins – AP-IMtofMS..... | 58 |
| b) Protein Mixtures – AP – IMtofMS..... | 62 |
| V. CONCLUSIONS..... | 63 |
| VI. ACKNOWLEDGMENTS..... | 64 |
| VII. REFERENCES..... | 65 |
| CHAPTER 4 | |
| I. CONCLUSIONS..... | 76 |

LIST OF TABLES

CHAPTER 2

Table 1: IMtofMS Operating Conditions Summary.....42

Table 2: Figure 3 (Anion Mixture) Peak Identities.....43

CHAPTER 3

Table 1 – AP-IMtofMS of Proteins.....68

LIST OF FIGURES

CHAPTER 2

Figure 1: A and B are 2D spectra of arsenic samples. A is 50ppm sodium arsenate solution, B is 50ppm sodium metaarsenite solution. Spectrum A shows the hydrogen arsenate ion ($\text{H}_2\text{AsO}_4^{-1}$ – 141 Da) and its fragment ion metaarsenate (AsO_3^-), corresponding to the loss of water. The metaarsenate ion is also present in solution, not as a fragment. Spectrum B, to which arsenate was not added, likewise shows these peaks. In addition, peaks corresponding to metaarsenite (AsO_2^-) and various arsenite/arsenate complexes are apparent in spectrum B.44

Figure 2 shows analysis of sulfate and phosphate. In these experiments sulfate is detected as HSO_4^- and phosphate as H_2PO_4^- , both of which have a mass of 97 Da. A shows sulfate data while B shows phosphate data. Note the presence of a 79 Da fragment ion, the result of a loss of water in spectrum A. Phosphate doesn't exhibit this loss of water. Spectrum C shows the separation of phosphate and sulfate via ion mobility – a distinction only possible by looking at the fragmentation pattern by MS alone.....45

Figure 3 shows a mixture of 2.5ppm NO_3 , 6.5ppm NO_2 , 70ppm Arsenate/Arsenite, 9ppm Cl, 30ppm H_2PO_4 and 15ppm HSO_4 . Note that only the metaarsenite sample was used as arsenate, arsenite and arsenate/arsenite complexes are present, as such a higher concentration is used. Unequal concentrations were an attempt to better equalize the resulting peak intensities. Spectrum A had the same experimental conditions as all previous experiments. Spectrum B better shows the resolving power potential of IMMS (around 100 for the mobility spectrum) by reducing the pulse width to 100us. However, the data acquisition time had to be increased to 60 minutes. Peaks A-O are identified in Table 2.....46

Figure 4 shows the results from real samples collected in the greater Seattle, WA, USA area. 4A is a background spectra, note the presence of nitrate, nitrite, chloride and sulfate in the background spectra. It was determined these were most probably due to contamination in the HPLC grade methanol. 4B shows a swamp creek sample and features corresponding to arsenate and arsenite are present in the spectrum. These results were not quantified. Figure 4C shows a sample collected on Washington Street, all features were present in the background, however, analytes of interest are present in the background. The analytes of interest in the Washington street sample seem to show increased intensities. Further work should be done with clean methanol.....47

CHAPTER 3

Figure 1: The 2D composite of mass and mobility data for porcine insulin showing baseline resolution of three porcine insulin charge states in both the mass and mobility domains. m/z values, charges states, drift times and reduced mobility values are identified for each peak. The sample was 200uM and collected at 200°C, 701 torr, 5uL/min, 441.1 V/cm for 30 minutes.....69

Figure 2 - The 2D composite of mass and mobility data for a 200uM sample of bovine insulin at 200°C, 689 torr, 5uL/min and 441.1 V/cm for 30 minutes. The spectrum shows baseline resolution of three insulin charge states in both the mass and mobility domains. Charge state, m/z value, drift time and reduced mobility are identified for all peaks.....70

Figure 3 - 2D composite spectrum of 200uM aprotinin collected at 200°C, 695 torr, 5uL/min and 441.1 V/cm for 30 minutes. The spectrum shows 5 peaks. One is identified as a fragment peak while the other four are identified as aprotinin charge states. Charge state (or designation as fragment), m/z value, drift time and reduced mobility are identified for all peaks present in the spectrum.....71

Figure 4 – 2D spectrum of mass and mobility for a 200uM sample of Cytochrome C taken at 200°C, 695 torr, 5uL/min and 441.1 V/cm for 60 minutes. The spectrum shows twelve peaks, all of which are identified as Cytochrome C charge states. One charge state (+8) is shown to have two conformations – hence two drift times.....72

Figure 5 – 2D spectrum of mass and mobility for 100 uM sample of Lysozyme collected at 250°C, 696 torr, 5uL/min and 441.1V/cm for 60 minutes. Ten features are evident: eight are Lysozyme charge states – one of which has two conformations drifting at different drift times, one feature is unidentified.....73

Figure 6 – 2D mass vs. mobility spectrum for a mixture of porcine and bovine insulin, both at 100uM concentration. Experimental conditions were 250°C, 698 torr, 5 uL/min and 441.1 V/cm for 30 minutes. Two mobilities are present representing 2 charge states. In the mass domain the bovine insulin peak is distinguishable from the porcine insulin peak with the same charge state, not so in the mobility domain.....74

Figure 7 – 2D spectrum, mass vs. mobility for a mixture of 130 uM Cytochrome C, 130 uM Lysozyme, 65 uM Aprotinin and 65uM Insulin at 200°C, 698 torr, 5 uL/min and 441.1 V/cm for 150 minutes. Proteins are shown to exhibit mass to mobility ratios that fall on compound specific trend lines. Trend lines can be used to quickly identify charge state peaks belonging to one protein or another.....75

CHAPTER 1

INTRODUCTION

I. IMS Background Information

a) Brief History

For roughly thirty five years, ion mobility spectrometry has been used as a method for trace organic analysis, specifically vapor phase detection, using radioactive ionization, of explosives, drugs and chemical warfare agents.¹ However, the breadth of experiments employing ion mobility spectrometry has been expanding with the use of electrospray ionization as an ionization source. In 1972 Dole and co-workers electrosprayed lysozyme into an ion mobility spectrometer producing three broad peaks.² The peaks were too broad to be useful and, consequently, effective use of ESI-IMS was delayed until, the late 1980's when Shumate and Hill³⁻⁵ successfully used electrospray in conjunction with corona discharge (calling it coronaspray) as a nebulization and ionization method for IMS, with increased sensitivity and stability. Since then electrospray ionization and MALDI have been used as ionization sources greatly increasing the applications of IMS to both solid and liquid phase analytes. These applications include but are not limited to narcotics,⁶ explosives,^{1,7,8} chemical warfare agents,^{9,10} carbohydrates,¹¹⁻¹⁵ peptides,¹⁶⁻²⁰ proteins,²¹⁻²³ oligonucleotides,²⁴⁻²⁵ and pesticides.²⁶⁻²⁷

b) How IMS works

Ion mobility spectrometry is a technique that separates ions based on their size to charge ratio. First a sample needs to be ionized. There are various ionization techniques employed in IMS. These techniques include radioactive ionization,^{1,28,29} photo-ionization,³⁰ surface ionization,³¹ secondary electrospray ionization,³² x-ray ionization,³³ and thermal or laser desorption.³⁴ While

radioactive ionization is commonly employed in commercial devices the most prevalent ionization source in IMS research is electrospray ionization first demonstrated by Shumate, et al.³⁻⁵ and later refined by Wittmer, et al.³⁵

Ionized ions enter a tube where a relatively weak, homogeneous electric field propels them towards the detector. In most modern designs the ions travel countercurrent to a neutral, heated drift gas. Most commonly the tube is formed via a stacked ring design.^{1,28} Alternating conductive and insulating rings of uniform size are stacked creating the tube. Conductive rings are connected via a resistor chain to which a potential is applied. This gradual, consistent reduction in potential produces the homogeneous electric field necessary to drive ions through the tube. Commonly the tube is divided into two distinct regions – a desolvation and a drift tube region. In the desolvation region ions travel in an uninterrupted ion stream through the heated drift gas where water molecules are stripped from the ions. Neutral contaminants and the stripped water molecules are carried out of the tube via the countercurrent flow of the drift gas. The desolvation and drift regions are separated by an ion gate, typically of a Bradbury-Nielson³⁶ style consisting of a wire grid made from two electrically isolated wires. “Closing” the gate is achieved by adjusting the potential difference between the wires above that of the electric field gradient in the tube. Ions are then caught in the electric field generated by the gate and neutralized. “Opening” the gate is a matter of setting the potential equal to that of the tube. Alternating rapidly between closed and open allows for the transfer of desolvated ion packets into the drift region of the ion mobility tube. Ions continue to travel down the potential gradient toward the detector. In the drift region ions of different types interact differently with the neutral drift gas based on their size and the polarizability of the drift gas. The overall effect is that the

progress through the tube is impeded more by the drift gas for some ions than for others and ions are effectively separated by type.

IMS instruments are operated at both low and high drift gas pressures. Low pressure systems operate with a drift gas pressure of approximately 2 torr and are employed by several research teams.³⁷⁻³⁹ Recently Smith, et al.⁴⁰ completed work experimenting with adjusting drift gas pressures from 4 to 12 torr seeing an increase in resolving power for the analysis of leucine enkephalin from 55 at 4 torr to 80 at 12 torr without significant loss in sensitivity. Still other research groups are operating IMS systems at atmospheric pressure. Wu, et al.⁴¹ reported resolving powers as high as 216 for the 11+ charge state of cytochrome c.

c) IMS Theory

As stated above, IMS separates analytes based on their interactions with the neutral drift gas.⁴² Separation of analytes is additionally influenced by diffusion due to the concentration gradient setup within the drift tube and, when applicable (like in the case of CO₂) to the polarizability of the drift gas.¹⁸ This degree to which an analyte interacts with the drift gas and consequently separates from other ions in the drift tube is known as its mobility (K). An ion's mobility is defined in terms of its average velocity through the drift tube (v_d) and the magnitude of the electric field (E), which can further be defined in terms of the length of the tube (L), the voltage drop through the drift region (V) and the average drift time of the analyte (t_d).

1)
$$K = \frac{v_d}{E} = \frac{L^2}{t_d V}$$

However, different instruments are operated at different temperatures (T) and pressures (P). To allow for comparability between instruments K_0 is used in the literature.

$$2) \quad K_0 = \frac{L^2}{t_d V} * \frac{P}{760} * \frac{273.15}{T}$$

K_0 values are the means by which analytes are identified in stand alone IMS experiments. The K_0 value for a given analyte should be the same regardless of the instrument or experimental conditions under which the mobility was determined and as such can be used to positively identify an analyte of interest as is done in with narcotics and explosives in airports on a daily basis. However, increasingly so, IMS is being used as a separations technique prior to mass spectrometry, where the actual identity of the analyte is determined via MS.

The degree to which an ion's progress through the drift tube is slowed by the drift gas depends on the average collision of an ion-drift gas (Ω), which is determined using the following equation:

$$3) \quad \Omega = \left[\frac{3}{16N_A} \right] \left[\frac{2\pi}{\mu kT} \right]^{1/2} \left[\frac{ze}{K} \right]$$

N_A is the number density of the drift gas in molecules per cm^3 – calculated as follows:

$N_A = \frac{P}{kT}$, where P is the pressure in atmospheres, k is Boltzmann's constant in $\text{L*atm}^\circ\text{K}$ and T

is the temperature in kelvin. μ is the reduced mass in kilograms of the ion(m)/neutral drift

gas(M) – defined as $\left(\frac{mM}{M+m} \right)$, k is the Boltzmann's constant in J°K , z is the charge of the ion, e

is the charge of an electron and K is the mobility of the ion in $\frac{\text{cm}^2}{\text{V*s}}$. Ions with the largest

collision cross section travel the slowest through the drift tube while ions with the smallest collision cross sections travel the fastest. One might think that since an ion's collision cross section is mass dependant an IMS is doing much the same thing as a mass spectrometer. However, isomers frequently have different collision cross sections and can therefore be separated by an IMS where a MS would be unable to differentiate between the two. This is where IMS exhibits its greatest strength and the reason IMS is quite frequently coupled with MS.

d) Ion Mobility Mass Spectrometry

The ability to differentiate isomers in an IMS and then identify them as such in a MS is one of the reasons this has become such a popular tandem instrumental technique. IMS has been successfully coupled with quadrupole,^{28,41,43-46} time-of-flight,^{22,47,48} quadrupole ion trap,^{38,49-51} linear ion trap²¹ and Fourier transform ion cyclotron resonance⁵² mass spectrometers. Typically in a tandem design the IMS comes before the MS. The IMS acts as a separations device similar to LC or GC with the advantage of faster experimental turn around times and in the case of GC without the need for volatile samples if ESI or one of the other aforementioned ionization techniques is employed. Also IMS is able to successfully separate isomers whereas in some cases the other separations techniques may not. In the case of the ion trap instruments the mass spectrometer typically is first in the tandem design, allowing for MSⁿ prior to IMS analysis of the fragments, again with one goal being the separation of isomeric fragment ions. In these designs the IMS must be operated at low (~2 torr) pressures due to interfacing problems with the ion traps. However, Clowers, et al.^{50,51} successfully coupled an atmospheric pressure IMS system before a quadrupole ion trap and were able to perform MSⁿ analyses on mobility selected ion populations.

II. Application of IMtofMS to Inorganic Contaminant Detection

a) Why Analyze for Inorganic Contaminants?

Although inorganic anions such as nitrate, nitrite, arsenate, and arsenite are ubiquitous environmental pollutants, they are difficult to detect and monitor. The primary sources of nitrate and nitrite environmental contamination are the excessive use of fertilizers, industrial waste streams and the biodegradation of nitrogenous biological material.⁵³ While nitrates and nitrites are ever present in the environment it has none the less been suggested that they're involved in infertility, the pathogenesis of methemoglobinemia, cancer, still birth in livestock, and tumors through a mechanism involving the formation of potentially mutagenic nitroso-compounds in the body.⁵⁴⁻⁵⁹ Arsenic can be found in food, air, soil and water. In water the primary forms of arsenic are inorganic ones. This is a problem as current evidence suggests the inorganic forms of arsenic are more acutely toxic than the organic ones. Arsenic exposure, primarily in from drinking water has been linked with skin and internal cancers, cardiovascular and neurological effects.⁶⁰

b) Current Analytical Practices

Currently standard analytical practices for the detection of nitrate and nitrite include spectrophotometry, cadmium reduction and ion chromatography.⁶¹ Standard analytical methods for arsenates and arsenites detection include graphite furnace atomic absorption spectrometry, gaseous hydride atomic absorption and anodic stripping voltammetry.⁶² Unfortunately, these methods cannot provide species information without some type of chromatographic separation prior to analysis. Methods of arsenate/arsenite detection approved by the EPA in drinking water include inductively coupled plasma-mass spectrometry and ICP-atomic emission spectrometry.

Other methods reported in the literature but not EPA approved include capillary electrophoresis, direct infusion electrospray ionization mass spectrometry (ESI-MS), high performance liquid chromatography inductively coupled plasma mass spectrometry (HPLC-ICP-MS), high performance liquid chromatography electrospray ionization mass spectrometry (HPLC-ESI-MS) and capillary electrophoresis electrospray ionization mass spectrometry (CE-ESI-MS).⁶²⁻⁶⁶ Detection limits for these and the EPA approved methods range from 0.5 ppb, for the single analyte GHAA method to 50 ppm for the ICP-AES and CE-ESI-MS methods (specifically for the inorganic As(III) species).

The viability of these techniques for on-site field measurements is limited due to their sensitivity to matrix effects, high cost, maintenance needs, low sensitivity and/or the requirement for extensive sample preparation prior to analysis. In addition, analysis time can be quite long. For today's environmental monitoring practices it is desirable that an instrument is fast, low cost, reliable, accurate, and sensitive. Furthermore, due to the possibility of contamination and the time delay between sample collection and analysis taking the instrument to the sample rather than the sample to the instrument is preferred, as such, it should be portable. Finally an analytical method should require minimal sample prep, offer the possibility for real time environmental monitoring and require minimal instrumental maintenance.

c) ESI-IMtofMS and Inorganic Contaminant Analysis

This work investigates the potential of electrospray ionization coupled with ion mobility spectrometry as a rapid but efficient analytical method for the determination of inorganic anions in aqueous samples. In 2002 by Dion, *et al.*⁶⁷ demonstrated the use of ESI-IMS for the detection

of inorganic analytes in aqueous media. Using several different cations, Dion demonstrated for the first time that IMS could be used for the separation and detection of inorganic ions. Recently, Dwivedi, et al⁶⁸ extended the use of IMS for the separation and detection of inorganic ions to anions by demonstrating that nitrate and nitrite anions could be separated and detected in river water samples. ESI-IMS's rapid analysis time, low detection limits and separation efficiency appeared to be ideal for separating and detecting inorganic anions in aqueous solutions.

Dion and Dwivedi used a stand alone IMS for their work and while it demonstrated the potential of IMS for the analytical determination of inorganic ions in aqueous samples, they were not able to identify the ions they were detecting. The use of an ion mobility time of flight mass spectrometer (IMtofMS) permits the two dimensional analysis of samples based on ion mobility and mass and the ability to separate isobaric compounds prior to mass analysis. In addition, random noise, both chemical and electronic, is separated in mobility space, increasing the signal/noise ratio in the mass spectrum.

Consequently the IM(tof)MS seems ideally suited to identifying the response ions which inorganic anions produce when they are electrosprayed from aqueous solutions into an ion mobility spectrometer. In particular, the work contained herein focuses on anions of environmental interest such as; nitrate, nitrite, sulfate, phosphate, arsenate, and arsenite.

III. Application of IMtofMS to Biomolecules

a) Why Analyze Biomolecules?

Biomolecules are of interest due to the ever increasing concern over the presence of biotoxins in the environment, be that presence the result of natural phenomenon or malicious intent. Online, rapid environmental monitoring for the presence of these large biomolecules is a potential application of IMS as a stand alone instrument. Due to the threat of bioterrorism, a rapid, online, field technique suitable to monitoring for the presence of biotoxins in aqueous media is of high demand in the world today. Furthermore, and unrelated to health concerns, the field of proteomics hinges on the ability to separate, detect and identify proteins in complex, biological matrices. While long acquisition times are less of a hindrance in the field of proteomics adequate separations of complex mixtures and the ability to accurately identify proteins is of the utmost importance.

b) IMS and IMMS Analysis of Individual Proteins

The IMS detection of proteins and their specific charge states was first demonstrated by Wittmer, et al. in 1994.³⁵ While this research focused on the implementation and improvement of electrospray ionization as the ionization source it nonetheless demonstrated for the first time detection of multiple protein charge states in an IMS – baseline resolution was absent, however, in this initial experiment. Cytochrome c has since been widely used in IMS and IMMS experiments, including but not limited to analysis by High-Field Asymmetric Waveform IMS (FAIMS),^{69,75} IMS,^{35,70,71} IM-QMS,⁷²⁻⁷⁴ IM(tof)MS,³⁹⁻⁴¹ FAIMS-IM-(tof)MS,⁷⁵ and Hadamard Transform IMS.⁷⁶ These Cytochrome c experiments have ranged in purpose, including probing

gas phase conformations of the charge states, use as a standard for improving ion mobility technique and monitoring structural changes in the ions throughout the course of the experiment.

The results of the aforementioned experiments along with other IMMS experiments of biomolecules have demonstrated many different benefits of a tandem IMMS experiment. Early in 1998 Clemmer *et al.*⁴⁸ reported the first IM(tof)MS data for biomolecules demonstrating simultaneous collection of data in both the mobility and mass domains, an advantage both in terms of data acquisition time and experimental complexity. Later that year, using an IM-QMS, Hill *et al.*⁴¹ achieved baseline resolution of Cytochrome c in the mobility domain for the first time. FAIMS-QMS and IM-QMS experiments cannot collect mobility and mass data simultaneously; consequently, they are typically operated in one of several modes: 1) The IMS can be “disabled” in an effort to collect a mass spectrum. 2) The MS can be “disabled,” acting simply as a detector to acquire a mobility spectrum. In the case of a FAIMS device this involves scanning across the band of voltages within the instrument. In the case of IMS this means pulsing the ion gate so that ions separate within the drift gas. 3) The FAIMS compensation voltage can be scanned while the MS is transmitting only one mass. A similar experiment can be performed with an IM-QMS instrument by pulsing the ion gate in the IMS and setting the quad to transmit only one mass. This experiment is useful for trying to identify isomers or different conformers of a given charge state since ions of the same mass can be detected with different mobilities. 4) With a FAIMS device one has the ability to selectively transmit only an ion of interest while the MS is scanned across the mass range. This can also be done with a traditional IMS instrument if a second ion gate is added just prior to leaving the drift tube as in Clowers’ experiment of 2005, employing the use on a quadrupole ion trap.⁵¹

c) IMMS Analysis of Protein Digests and CID

IMMS work, as it relates to proteins, has also focused on MS/MS protein/peptide fragmentation experiments and protein digests. The use of IMS to separate the resulting peptides has proved to be very useful and there are many, many examples of said work in the literature. However, the novel work being reported herein focuses on the use of ESI-IMS to separate mixtures of intact proteins. As such, a select few examples of separations of peptide mixtures, via protein digest or CID, are included here in an effort to recognize this important on going work in a related field of study.

The ability to separate peptide mixtures resulting from protein digests or CID has been demonstrated in several experiments. Some of these include ion trap-MS/MS-IM-(tof)MS analysis of Ubiquitin and Insulin,^{77,78} Nano-LC-IMS-(tof)MS analysis of *Drosophila* protein extract digest,⁷⁹ Nano-LC-IM-CID-(tof)MS analysis of the digest of soluble proteins extracted from human urine,⁸⁰ ESI-FAIMS-MS analysis of a tryptic digest of pig hemoglobin,⁸¹ Nano-LC-FAIMS-MS,⁸² and IMS-IMS or IMS-IMS-IMS/MS of peptide and protein fragments.⁸³⁻⁸⁵ The insulin and ubiquitin works are discussed herein because they exhibit two different approaches to peptide analysis of proteins that have undergone CID using IMMS. The first type of experiment illustrated in this work⁷⁸ is one where the instrument was set up so that ion mobility separation of a given charge state precedes, CID and finally TOF-MS. This instrumental arrangement allows for MS/MS analysis of the different conformations (as indicated by the IMS portion of the experiment) of one protein charge state. Note that in this instrumental arrangement the ion

mobility apparatus was being used for separation of the various intact protein charge state spatial conformations prior to fragmentation or mass analysis.

The insulin and other ubiquitin⁷⁷ work shows m/z identification and isolation of one protein charge state and fragmentation prior to determination of ion mobilities. As such, in these experiments the ion mobility is being used to help separate peptide fragment ions prior to TOF-MS, intact proteins never enter the drift region of the instrument. The result was the identification of charge state families where protein fragments with the same charge state fell on identifiable trend lines within the m/z vs. drift time data.

Clemmer's work with protein digests (*Drosophila* and the human urinary proteome) added a nano-LC to an IMS-TOF instrument. In both instances mass spectral analysis, be it MS/MS or MS, happened after separation via nano-LC and IMS. These two degrees of separation allow for better resolving of the individual peptides analyzed in their work. In both these examples the spectra are incredibly complicated but identification of many features are possible by singling in on specific LC retention times/IMS drift times then looking at the MS/MS spectra.

Peptide mixtures have also been analyzed using FAIMS-MS techniques and again the work discussed herein is just one example of many in the field. The analysis of a tryptic digest of pig hemoglobin using ESI-FAIMS-MS⁸¹ is similar to previously discussed FAIMS work where the FAIMS device acts as a filter prior to mass analysis. Since only a portion of the peptides present in a sample are transmitted at any given moment, scanning the compensation voltage of the FAIMS device reduces the number of ions detected by the MS allowing for better resolution and

mass identification of species present in the sample. As with IMMS, nano-LC has been coupled with FAIMS/MS for the analysis of a protein digest.⁸² While the use of the FAIMS device is similar to the aforementioned experiment the addition of the nano-LC resulted in a reduction in spectral complexity.

Finally, the use of tandem IMS as a stand alone technique or coupled with MS has also been successfully implemented in the analysis of peptide and protein fragment ions.⁸³⁻⁸⁵ In these experiments certain charge states can be selected in the first IMS, fragmented and then passed on to a second IMS where these fragments and/or ion rearrangements are further separated. At this point in the experiment ions are either detected⁸³⁻⁸⁵ or the process is repeated in a third IMS then ions are transferred into a MS for mass analysis.⁸³ The benefit of this technique has been an increase in peak capacity from ~60-80 up to ~480-1360. Many features of a spectra not readily apparent via MS alone become apparent through the application of tandem IMS.

d) Protein Mixtures

While the above work has firmly cemented IMS as a useful tool in proteomics the intended goal of this researcher is to show the potential of ESI-IMS as a separations technique for mixtures of intact proteins. Very little work has been done with the separation of intact proteins in a mixture using IMS. Clemmer, *et al.*²¹ have analyzed protein mixtures using a nano-LC/IMS-MS instrument. However, the primary means of protein separation in these experiments is the nano-LC. Therefore the analysis of intact proteins was carried out through successful separation in the following order: a mixture of intact proteins using LC, charge state conformers using IMS and m/z values using MS.

Smith *et al.*⁸⁶ analyzed a mixture of thirty proteins and peptides using an ESI-FAIMS/IMS/Q-TOF-MS instrument. Sixteen FAIMS compensation voltages were selected and used as ion filters. IMMS spectra were then collected for each of the 16 CV's. The FAIMS filtering markedly decreased the spectral complexity of the IMMS spectra, leading to easier identification of peaks. In essence the FAIMS device and IMS device were used collectively as a separations step prior to mass analysis. This is by far the most similar experiment to that proposed herein, with the exception that IMS is proposed as the sole separations technique prior to MS. Toward that end a simpler protein mixture will be employed in this preliminary investigation into the usefulness of IMS as the sole protein separations step prior to MS.

IV. Specific Aims

IMS as a stand alone instrument is a portable, low cost, low maintenance instrument ideally suited for field measurements. However, prior to its application as such it was necessary to precisely identify masses of species that are detected at an experimentally determined mobility value. To this end, inorganic environmental contaminants (Specific Aim 1) were analyzed using ESI-IM(tof)MS. Due to the potential for complexing and interaction between various species in a mixture the analysis of said mixture was necessary so these mobility peaks could likewise be mass identified. (Specific Aim 2)

Portable instruments are also desired for the detection of biotoxins in aqueous media and with that goal in mind proteins were analyzed individually in an effort to mass identify observed mobility peaks (Specific Aim 3). Similar to the work with inorganic environmental contaminants, real world analysis of proteins means analyzing protein mixtures; therefore, a protein mixture was analyzed as part of this study. While performing this work it was realized that, in addition to environmental monitoring, a significant need for the separation of proteins lies in the field of proteomics. Consequently, the viability of IMS as a protein separations technique, under the umbrella of proteomics research, was also investigated. (Specific Aim 4)

1. Mass identify the mobility peaks present when analyzing individual inorganic anions in aqueous media using ESI-IMS. – Chapter 2
2. Mass identify the mobility peaks present when analyzing inorganic anion mixtures using ESI-IMS and compare to those observed in individual experiments. – Chapter 2

3. Mass identify the mobility peaks present when analyzing individual proteins found in aqueous samples using ESI-IMS in order to test the viability of ESI-IMS as a portable field instrument for the detection of biotoxins in the environment. – Chapter 3
4. Investigate the effectiveness of IMS as a separations technique prior to MS for the analysis of protein mixtures. – Chapter 3

REFERENCES

1. Eiceman, G.A.; Karpas, Z. *Ion Mobility Spectrometry*; CRC Press: Boca Raton, FL, **1994**.
2. Gieniec, M.L.; Cox, J., Jr.; Teer, D.; Dole, M. *20th Annual Conference on Mass Spectrometry and Allied Topics*, Dallas, TX. June 4-9, 1972.
3. Shumate, C.B.; Hill, H.H., Jr. Northwest Regional ACS Meeting, Bellingham WA, June **1987**
4. Shumate, C.B. *An Electrospray/Nebulization/Ionization Interface for Liquid Introduction into an Ion Mobility Spectrometer* Ph.D. Thesis, Washington State University, **1989**.
5. Shumate, C.B.; Hill, H.H., Jr. *Coronaspray nebulization and ionization of liquid samples for ion mobility spectrometry*. *Anal. Chem.* **1989**, 61, 601-606.
6. Matz, L.M.; Hill, H.H., Jr. *Evaluation of Opiate Separation by High-Resolution Electrospray Ionization – Ion Mobility Spectrometry/Mass Spectrometry*. *Anal. Chem.* **2001**, 73(8), 1664-1669.
7. Asbury, G. R.; Klasmeier, J.; Hill, H. H., Jr. *Analysis of explosives using electrospray ionization/ion mobility spectrometry (ESI/IMS)*. *Talanta* **2000**, 50(6), 1291-1298.
8. Buxton, T. L.; Harrington, P. de B. *Trace explosive detection in aqueous samples by solid-phase extraction ion mobility spectrometry (SPE-IMS)*. *Appl. Spectr.* **2003**, 57(2), 223-232.
9. Steiner, W.E.; Clowers, B.H.; Matz, L.M.; Siems, W.F.; Hill, H.H., *Rapid Screening of Aqueous Chemical Warfare Agent Degradation Products: Ambient Pressure Ion Mobility Mass Spectrometry (IMMS)*, *Anal. Chem.* **2002**, 74, 4343-4352.
10. Steiner, W. E.; Clowers, B. H.; Haigh, P. E.; Hill, H. H. *Secondary Ionization of Chemical Warfare Agent Simulants: Atmospheric Pressure Ion Mobility Time-of-Flight Mass Spectrometry*. *Anal. Chem* **2003**, 75(22), 6068-6076.
11. Lee, S.; Wytenbach, T.; Bowers, M. T.. *Gas phase structures of sodiated oligosaccharides by ion mobility/ion chromatography methods*. *Int. J. Mass Spec. Ion Proc.* **1997**, 167/168, 605-614.
12. Liu, Y. and Clemmer, D.E. *Characterizing oligosaccharides using injected-ion mobility/mass spectrometry*. *Anal. Chem.* **1997**, 69, 2504-2509.
13. Lee, D.-S., Wu, C. and Hill, H.H., *Detection of carbohydrates by electrospray ionization-ion mobility spectrometry following microbore high-performance liquid chromatography*. *J. Chromatog., A.*, **1998**, 822, 1-9.
14. Leavell, M. D.; Gaucher, S. P.; Leary, J. A.; Taraszka, J. A.; Clemmer, D. E.. *Conformational studies of Zn-ligand-hexose diastereomers using ion mobility measurements and density functional theory calculations*. *J. Am. Soc. Mass Spec.* **2002**, 13(3), 284-293.
15. Clowers, B.H.; Bendiak, B.; Dwivedi, P.; Steiner, W.E.; Hill, H.H. Jr. *Separation of Sodiated Isobaric Disaccharides Using Electrospray Ionization-Atmospheric Pressure Ion Mobility-Time of Flight Mass Spectrometry*. *J. Am. Soc. Mass Spec.* **2005**, 16, 660-669.
16. Wu, C.; Siems, W. F.; Klasmeier, J.; Hill, H. H. Jr.. *Separation of Isomeric Peptides Using Electrospray Ionization/High-Resolution Ion Mobility Spectrometry*. *Anal. Chem.* **2000**, 72 391-395.
17. Srebalus-Barnes, C. A.; Hilderbrand, A. E.; Valentine, S. J.; Clemmer, D. E.. *Resolving Isomeric Peptide Mixtures: A Combined HPLC/Ion Mobility-TOFMS Analysis of a 4000-Component Combinatorial Library*. *Anal. Chem.* **2002**, 74, 26-36.

18. Hill, Herbert H.; Hill, Chandler H.; Asbury, G. Reid; Wu, Ching; Matz, Laura M.; Ichiye, Toshiko. *Charge location on gas phase peptides*. Int. J. Mass Spec. **2002**, 219(1), 23-37.
19. Ruotolo, B. T.; Verbeck, G. F., IV; Thomson, L. M.; Woods, A. S.; Gillig, K. J.; Russell, D. H. *Distinguishing between phosphorylated and nonphosphorylated peptides with ion mobility-mass spectrometry*. J. of Prot. Res. **2002**, 1(4), 303-306.
20. Breaux, G. A.; Jarrold, M. F. *Probing Helix Formation in Unsolvated Peptides*, J. Am. Chem. Soc., **2003**, 125, 10740-10747.
21. Sowell, R. A.; Koeniger, S. L.; Valentine, S. J.; Moon, M. H.; Clemmer, D. E. *Nanoflow LC/IMS-MS (and – CID/MS) of Protein Mixtures*, J. Am. Soc. Mass Spectrom. **2004**, 15, 1341-1353.
22. Ruotolo, B. T.; Gillig, K. J.; Stone, E. G.; Russell, D. H.; Fuhrer, K.; Gonin, M.; Schultz, J. A.. *Analysis of protein mixtures by matrix-assisted laser desorption ionization-ion mobility-orthogonal-time-of-flight mass spectrometry*. Int. J. Mass Spec. **2002**, 219(1), 253-267.
23. Bernstein S. L.; Wyttenbach T.; Baumketner A.; Shea, J. E.; Bitan, G.; Teplow, D. B.; Bowers, M. T., *Amyloid β -Protein: Monomer Structure and Early Aggregation States of A β 42 and Its Pro19 Alloform*. J. Am. Chem. Soc. **2005**, 127, 2075-2084.
24. Koomen, J. M.; Ruotolo, B. T.; Gillig, K. J.; McLean, J. A.; Russell, D. H.; Kang, M.; Dunbar, K. R.; Fuhrer, K.; Gonin, M.; Schultz, J. A.. *Oligonucleotide analysis with MALDI-ion-mobility-TOFMS*. Anal. Bioanal. Chem. **2002**, 373(7), 612-617.
25. Gidden, J.; Baker, E. S.; Ferzoco, A.; Bowers, M. T. *Structural Motifs of DNA Complexes in the Gas Phase*. Int. J. Mass Spec. **2005**, 240, 183-193.
26. Clowers, B.H.; Steiner, W.E.; Dion, H.M.; Matz, L.M.; Tam, M.; Tarver, E.E.; Hill, H.H., *Evaluation of Sulfonyleurea Herbicides Using High Resolution Electrospray Ionization-Ion Mobility-Quadrupole Mass Spectrometry*, Field Anal. Chem. Tech., **2001**, 5(6), 302-312.
27. Dion, Heather M. *Determination of distribution coefficients for polar herbicides*. (Dissertation) **2001**, 155 pp.
28. Karasek, F. W.; Kim, S. H.; Hill, H. H. Jr. *Mass Identified Mobility Spectra of p-Nitrophenol and Reactant Ions in Plasma Chromatography*, Anal. Chem., **1976**, 48(8), 1133-1137.
29. Karasek, F. W.; Hill, H. H. Jr.; Kim, S. H.. *Plasma Chromatography of Heroin and Cocaine with Mass-Identified Mobility Spectra*, J. Chromatogr., **1976**, 117, 327-336.
30. Baim, M.A., Eatherton, R.L., Hill, H.H. *Ion mobility detector for gas chromatography with a direct photoionization source*. Anal. Chem. **1983**, 55, 1761-1766.
31. Wu, C., Hill, H.H., Rasulev, U.K., Nazarov, E.G. *Surface ionization ion mobility spectrometry*. Anal. Chem. **1999**, 71, 273-278.
32. Wu, C., Siems, W.F., Hill, H.H. *Secondary Electrospray Ionization Ion Mobility Spectrometry/Mass Spectrometry of Illicit Drugs*. Anal. Chem. **2000**, 72, 396-403.
33. Pershenkov, V.S., Tremasov, A.D., Belyakov, V.V., Razvalyaev, A.U., Mochkin, V.S. *X-ray Ion Mobility Spectrometer*. Microelectronics and Reliability, In Press, Corrected Proof.
34. Tabrizchi, M. *Thermal Ionization Ion Mobility Spectrometry of Alkali Salts*. Anal. Chem. **2003** 75(13), 3101-3106.

35. Wittmer, D.; Chen, Y. H.; Luckenbill, B. K.; Hill, H. H., Jr. *Electrospray Ionization Ion Mobility Spectrometry*. *Anal. Chem.* **1994**, 66(14), 2348-55.
36. Bradbury, N. E.; Nielsen, R. A. *Absolute values of the electron mobility in hydrogen*. *Physical Rev.* **1936**, 49, 388-93.
37. Shaffer, S.A., Tolmachev, A., Prior, D.C., Anderson, G.A., Udseth, H.R., Smith, R.D. *Characterization of an Improved Electrodynamic Ion Funnel Interface for Electrospray Ionization Mass Spectrometry*. *Anal. Chem.* **1999**, 71, 2957-2964.
38. Valentine, S.J., Counterman, A.E., Clemmer, D.E. *Conformer-Dependent Proton-Transfer Reaction of Ubiquitin Ions*. *J. Am. Soc. Mass Spec.* **1997**, 8, 954-961.
39. Thalassions, K., Slade, S.E., Jennings, K.R., Scrivens, J.H., Giles, K., Wildgoose, J., Hoyes, J., Bateman, R.H., Bowers, M.T. *Ion Mobility Mass Spectrometry of Proteins in a Modified Commercial Mass Spectrometer*. *Int. J. of Mass. Spec.* **2004** 236, 55-63.
40. Baker, E.S., Clowers, B.H., Li, F., Tang, K., Tolmachev, A.V., Prior, D.C., Belov, M.E., Smith, R.D. *Ion Mobility Spectrometry-Mass Spectrometry Performance Using Electrodynamic Ion Funnels and Elevated Drift Gas Pressures*. **2007**, *J. Am. Soc. Mass Spec.* 18, 1176-1187.
41. Wu, C.; Siems, W. F.; Asbury, G. R.; Hill, H. H., Jr. *Electrospray Ionization High-Resolution Ion Mobility Spectrometry-Mass Spectrometry*. *Anal. Chem.* **1998**, 70(23), 4929-4938.
42. Revercomb, H. E.; Mason, E. A. *Theory of plasma chromatography/gaseous electrophoresis*. *Anal. Chem.* **1975**, 47(7), 970-83.
43. Liu, Y.; Valentine, S. J.; Counterman, A. E.; Hoaglund, C. S.; Clemmer, D. E. *Injected-ion Mobility Analysis of Biomolecules*. *Anal. Chem.* **1997**, 69, 728A.
44. Wyttenbach, T.; Kemper, P. R.; Bowers, M. T. *Design of a New Electrospray Ion Mobility Mass Spectrometer* *Int. J. Mass Spec.* **2001**, 212, 13.
45. Hudgins, R. R.; Woenckhaus, J.; Jarrold, M. F. *High Resolution Ion Mobility Measurements for Gas Phase Proteins: Correlation between Solution Phase and Gas Phase Conformations*, *Int. J. Mass Spec. Ion Proc.*, **1997**, 165/166, 497-507.
46. Dugourd, P.; Hudgins, R. R.; Clemmer, D. E.; Jarrold, M. F. *High Resolution Ion Mobility Spectrometer*. *Rev. Sci. Instrum.* **1997**, 68 (2), 1122-1129.
47. Steiner, W. E.; Clowers, B. H.; Fuhrer, K.; Gonin, M.; Matz, L. M.; Siems, W. F.; Schultz, A. J.; Hill, H. H. Jr., *Electrospray Ionization With Ambient Pressure Ion Mobility Separation And Mass Analysis By Orthogonal Time-of-Flight Mass Spectrometry*, *Rapid Comm. in Mass Spec.*, **2001**, 15 (23), 2221-2226.
48. Hoaglund, C. S.; Valentine, S. J.; Sporleder, C. R.; Reilly, J. P.; Clemmer, D. E. *Three-Dimensional Ion Mobility/TOFMS Analysis of Electrosprayed Biomolecules*, *Anal. Chem.* **1998**, 70, 2236-2242.
49. Creaser, C. S.; Benyazzar, M.; Griffiths, J. R.; Stygall, J. W. *A Tandem Ion Trap/Ion Mobility Spectrometer*. *Anal. Chem.* **2000**, 72(13), 2724-2729.
50. Clowers, Brian H.; Hill, Herbert H., Jr. *Influence of cation adduction on the separation characteristics of flavonoid diglycoside isomers using dual gate-ion mobility-quadrupole ion trap mass spectrometry*. *Journal of Mass Spectrometry* (2006), 41(3), 339-351.
51. Clowers, Brian H.; Hill, Herbert H., Jr. *Mass Analysis of Mobility-Selected Ion Populations Using Dual Gate, Ion Mobility, Quadrupole Ion Trap Mass Spectrometry*. *Analytical Chemistry* (2005), 77(18), 5877-5885.

52. Bluhm, B. K.; Gillig, K. J.; Russell, D. H.. *Development of a Fourier-transform ion cyclotron resonance mass spectrometer-ion mobility spectrometer*. Rev. Sci. Instrum. **2000**, 71(11), 4078-4086.
53. Peyton, B.M.; Peterson, J.N. Water Res. **2001**, 35, 215-231.
54. Weisburger, J.H. *Role of fat, fiber, nitrate, and food additives in carcinogenesis: a critical evaluation and recommendations*. Nutr. Cancer, **1986**, 8, 47-62.
55. Carson, T.L. *Vet. Clin. North. Am. Food. Anim. Pract.*, **2000**, 16, 455-464.
56. Connolly, D. *Rapid determination of nitrate and nitrite in drinking water samples using ion-interaction liquid chromatography*. Anal. Chim. Acta, **2001**, 441, 53-62.
57. W.H.O. *Tech. Rep. Ser.*, **1995**, 859, 1-54.
58. Oldreive, C.; Rice-Evans, C. *The mechanisms for nitration and nitrotyrosine formation in vitro and in vivo: impact of diet*. Free Radical Res., **2001**, 35, 215-231.
59. Graham, E. *Clin. Biochem* **1998**, 31, 195-220.
60. Abernathy, C.O.; Liu, Y.; Longfellow, D.; Aposhian, H.V.; Beck, B.; Fowler, B.; Goyer, R.; Menzer, R.; Rossman, T.; Thompson, C.; Waalkes, M. *Arsenic: health effects, mechanisms of actions, and research issues*. Env. Health Pers. **1999**, 107(7), 593-597.
61. Greenberg, A.E.; Clesceri, L.S.; Eaton, M.A. *American Public Health Association*, 18th edition, **1992**, 1-4.
62. Office of Ground Water and Drinking Water Standards and Risk Management Division, U.S. EPA, EPA-815-R-00-010, **1999**
63. Forte, G.; Amato, D.; Caroli, S. *A pilot study on the contents of selected pollutants in fish from the Tiber River (Rome)*. Microchem. Journal, **2005**, 15-19.
64. Florencio, M.H.; Duarte, M.F.; Bettencourt, A.M.M.; Bomes, M.L.; Vilas Boas, L.F. *Electrospray mass spectra of arsenic compounds*. Rapid Comm. in Mass Spec. **1997**, 11, 469-473.
65. Schramel, O.; Michalke, B.; Kettrup, A. *Application of capillary electrophoresis-electrospray ionisation mass spectrometry to arsenic speciation*. J. Anal. At. Spec. **1999**, 14, 1339-1342.
66. McSheehy, S.; Szpunar, J.; Lobinski, R.; Haldys, V.; Tortajada, J.; Edmonds, J.S. *Characterization of Arsenic Species in Kidney of the Clam *Tridacna derasa* by Multidimensional Liquid Chromatography-ICPMS and Electrospray Time-of-Flight Tandem Mass Spectrometry*. Anal. Chem. **2002**, 74, 2370-2378.
67. Dion, H.M.; Ackerman, L.K.; Hill, H.H. *Detection of inorganic ions from water by electrospray ionization-ion mobility spectrometry*. Talanta, **2002**, 57, 1161-1171.
68. Dwivedi, P.; Matz, L.M.; Atkinson, D.A.; Hill, H.H. *Electrospray Ionization-Ion Mobility Spectrometry: A Rapid Analytical Method for Aqueous Nitrate and Nitrite Analysis*. Analyst **2004**, 129, 139-144.
69. Shvartsburg, Alexandre A.; Bryskiewicz, Tadeusz; Purves, Randy W.; Tang, Keqi; Guevremont, Roger; Smith, Richard D. *Field Asymmetric Waveform Ion Mobility Spectrometry Studies of Proteins: Dipole Alignment in Ion Mobility Spectrometry?* Journal of Physical Chemistry B **2006**, 110(43), 21966-21980.
70. Clemmer, D.E., Hudgins, R.R., Jarrold, M.F. *Naked Protein Conformations: Cytochrome c in the Gas Phase*. **1995** J. Am. Chem. Soc. 117, 10141-10142.

71. Badman, E.R., Myung, S., Clemmer, D.E. *Evidence for Unfolding and Refolding of Gas-Phase Cytochrome c Ions in a Paul Trap*. J. Am. Soc. Mass Spec. **2005** 16, 1493-1497.
72. Matz, L.M., Steiner, W.E., Clowers, B.H., Hill, H.H. *Evaluation of Micro-Electrospray Ionization with Ion Mobility Spectrometry/Mass Spectrometry*. Int. J. of Mass Spec. **2002**, 213, 191-202.
73. Shelimov, K.B., Clemmer, D.E., Hudgins, R.R., Jarrold, M.F. *Protein Structure in Vacuo: Gas-Phase Conformations of BPTI and Cytochrome c*. J. Am. Chem. Soc. **1997**, 119, 2240-2248.
74. Badman, E.R., Hoaglund-Hyzer, C.S., Clemmer, D.E. *Monitoring Structural Changes of Proteins in an Ion Trap over ~10-200ms: Unfolding Transitions in Cytochrome c Ions*. Anal. Chem. **2001**, 73, 6000-6007.
75. Shvartsburg, A.A., Li, F., Tang, K., Smith, R.D. *Characterizing the Structures, and Folding of Free Proteins Using 2-D Gas-Phase Separations: Observation of Multiple Unfolded Conformers*. Anal. Chem. **2006**, 78, 3304-3315.
76. Clowers, B.H., Siems, W.F., Hill, H.H., Massick, S.M. *Hadamard Transform Ion Mobility Spectrometry*. Anal. Chem. **2006**, 78, 44-51.
77. Badman, E.R., Myung, S., Clemmer, D.E. *Gas-Phase Separations of Protein and Peptide Ion Fragments Generated by Collision-Induced Dissociation in an Ion Trap*. Anal. Chem. **2002**, 74, 4889-4894.
78. Badman, E.R.; Hoaglund-Hyzer, C.S.; Clemmer, D.E. *Dissociation of Different Conformations of Ubiquitin Ions*. J. Am. Soc. Mass Spectrom. **2002**, 13, 719-723.
79. Myung, S.; Lee, Y.L.; Moon, M.H.; Taraszka, J.; Sowell, R.; Koeniger, S.; Hilderbrand, A.E.; Valentine, S.J.; Cherbas, L.; Cherbas, P.; Kaufmann, T.C.; Miller, D.F.; Mechref, Y.; Novotny, M.V.; Ewing, M.A.; Sporleder, C.R.; Clemmer, D.E. *Development of High-Sensitivity Ion Trap Ion Mobility Spectrometry Time-of-Flight Techniques: A High-Throughput Nano-LC-IMS-TOF Separation of Peptides Arising from a Drosophila Protein Extract*. Anal. Chem. **2003**, 75, 5137-5145.
80. Moon, M.H.; Myung, S.; Plasencia, M.; Hilderbrand, A.E.; Clemmer, D.E. *Nanoflow LC/Ion Mobility/CID/TOF for Proteomics: Analysis of a Human Urinary Proteome*. J. of Proteome Research. **2003**, 2, 589-597.
81. Guevremont, R.; Barnett, D.A.; Purves, R.W.; Vandermeij, J. *Analysis of a Tryptic Digest of Pig Hemoglobin Using ESI-FAIMS-MS*. Anal. Chem. **2000**, 72, 4577-4584.
82. Venne, K.; Bonneil, E.; Eng, K.; Thibault, P. *PharmaGenomics*. **May 2004**, 31-40.
83. Merenbloom, S.I., Koeniger, S.L., Valentine, S.J., Plasencia, M.D., Clemmer, D.E. *IMS-IMS and IMS-IMS-IMS/MS for Separating Peptide and Protein Fragment Ions*. Anal. Chem. **2006**, 78, 2802-2809.
84. Koeniger, S.L., Merenbloom, S.I., Valentine, S.J., Jarrold, M.F., Udseth, H.R., Smith, R.D., Clemmer, D.E. *An IMS-IMS Analogue of MS-MS*. Anal. Chem. **2006**, 78, 4161-4174.
85. Merenbloom, S.I., Bohrer, B.C., Koeniger, S.L., Clemmer, D.E. *Assessing the Peak Capacity of IMS-IMS Separations of Tryptic Peptide Ions in He at 300K*. Anal. Chem. **2007**, 79, 525-522.
86. Tang, K.; Li, F.; Shvartsburg, A.A.; Strittmatter, E.F.; Smith, R.D. *Two-Dimensional Gas-Phase Separations Coupled to Mass Spectrometry for Analysis of Complex Mixtures*. Anal. Chem. **2005**, 77 – 19, 6381 – 6388.

CHAPTER 2

Determination of Inorganic Anions in Aqueous Samples by Ion Mobility Time-of-Flight Mass Spectrometry (IMtofMS)

By

Steven J. Klopsch, Brian H. Clowers, Wes E. Steiner and Herbert H. Hill*.

Department of Chemistry

Washington State University

Pullman, WA 99164-4630

Tel: (509) 335-5648

Fax: (509) 335-8867

E-mail: hhill@wsu.edu

To be Submitted to

International Journal of Ion Mobility Spectrometry

*** to whom correspondence should be addressed**

ABSTRACT

An ion mobility time-of-flight mass spectrometer was used to demonstrate the potential of ion mobility spectrometry for the rapid analysis of inorganic anionic environmental contaminants in aqueous samples. While baseline resolution for a mixture of seven inorganic anions was achieved in the mobility domain, this work also demonstrated the power of two dimensional separations based on ion mobility and mass spectrometry. For example, isobaric sulfate and phosphate ions could not be separated by their mass but could be separated by mobility. Similarly, unresolved peaks that could not be separated by ion mobility could be resolved by mass spectrometry. Separation and the subsequent identification of peaks in both standard and real world samples are reported.

KEYWORDS

Ion Mobility Spectrometry, Time-of-Flight Mass Spectrometry, Inorganic Anions.

INTRODUCTION

Although inorganic anions such as nitrate, nitrite, sulfate, phosphate, arsenate, and arsenite are ubiquitous environmental pollutants, they are difficult to detect and monitor. Nitrate and nitrite contaminate the environment by the excessive use of fertilizers, industrial waste streams (explosives, pharmaceuticals and food processing) and the biodegradation of nitrogenous biological material.¹ It has been suggested that nitrate and nitrite are involved in infertility, the pathogenesis of methemoglobinemia, cancer, still birth in livestock, and tumors through a mechanism involving the formation of potentially mutagenic nitroso-compounds in the body.²⁻⁷ Arsenic is present in food, soil, air and water. The primary forms of arsenic in water are inorganic and current evidence suggests the inorganic forms are more acutely toxic than the organic ones. Skin and internal cancers, cardiovascular and neurological effects have been attributed to arsenic exposure, mainly from drinking water.⁸

Sulfate and phosphate are common in the environment and naturally occurring. The health risk of sulfate and phosphate to humans is negligible and consequently neither is controlled by the EPA's drinking water standards. Sulfate was included on the EPA's "contaminant candidate list" of 1998 but it was deemed that no regulatory action was needed in 2003. Phosphate has never been regulated by the EPA with regards to safe water, however, it is a significant cause of eutrophication in bodies of water around the world. Eutrophication can lead to excessive plant growth and decay, which can further lead to decreased oxygen content, impact and fish/animal populations and diminished water quality. The ability to detect sulfate and phosphate in water is important for monitoring the effects widespread fertilization and pesticide use is having on local

fish and animal populations. It's also important to understand instrumental response to phosphate and sulfate due to their ever presence in water samples and their potential for interference when monitoring other regulated water contaminants.

Currently standard analytical practices for the detection of nitrate and nitrite include spectrophotometry, cadmium reduction and ion chromatography.⁹ The applicability of these techniques to on-site field measurements can be limited by interference from matrix effects, low sensitivity and/or the requirement for extensive sample preparation prior to analysis. In addition, analysis time can be quite long. For today's environmental monitoring practices it is desirable that an instrument is fast, low cost, reliable, accurate, and sensitive. Furthermore, due to the possibility of contamination and the time delay between sample collection and analysis taking the instrument to the sample rather than the sample to the instrument is preferred, as such, it should be portable. Finally an analytical method should require minimal sample prep, offer the possibility for real time environmental monitoring and require minimal instrumental maintenance.

Standard analytical methods for arsenates and arsenites have similar disadvantages. They include the detection of arsenate and arsenites by graphite furnace atomic absorption spectrometry, gaseous hydride AA and anodic stripping voltammetry.¹⁰ Unfortunately, these methods cannot provide species information without some type of chromatographic separation prior to analysis. EPA approved methods for detection of arsenates and arsenites in drinking water include inductively coupled plasma-mass spectrometry and ICP-atomic emission spectrometry. Other methods used for arsenic analysis which have been reported in the literature

but are not EPA approved include capillary electrophoresis, direct infusion electrospray ionization mass spectrometry (ESI-MS), high performance liquid chromatography inductively coupled plasma mass spectrometry (HPLC-ICP-MS), high performance liquid chromatography electrospray ionization mass spectrometry (HPLC-ESI-MS) and capillary electrophoresis electrospray ionization mass spectrometry (CE-ESI-MS).¹¹⁻¹⁴ Detection limits for these and the EPA approved methods range from 0.5 ppb, for the single analyte GHAA method to 50 ppm for the ICP-AES and CE-ESI-MS methods (specifically for the inorganic As(III) species).

This work investigates the potential of electrospray ionization coupled with ion mobility spectrometry as a rapid but efficient analytical method for the determination of inorganic anions in aqueous samples. Electrospray ionization ion mobility spectrometry (ESI-IMS) was first reported by Shumate and Hill¹⁵ in the late 1980's, which lead to work with peptides, proteins and other non-volatile compounds in aqueous media. The detection of proteins and separation of charge states was first demonstrated by Wittmer, *et al.*¹⁶ in 1994. However, the detection of inorganic analytes in aqueous media via ESI-IMS wasn't reported until 2002 by Dion, *et al.*¹⁷.

Using several different cations, Dion demonstrated for the first time that IMS could be used for the separation and detection of inorganic ions. Recently, Dwivedi, *et al.*¹⁸ extended the use of IMS for the separation and detection of inorganic ions to anions by demonstrated that nitrate and nitrite anions could be separated and detected in river water samples. ESI-IMS appeared to be an ideal method for separating and detecting inorganic anions in aqueous solutions due to its rapid analysis time, high separation efficiency and low detection limits.

While the work of Dion and Dwivedi demonstrated the potential of IMS for the analytical determination of inorganic ions in aqueous samples, they used a stand alone IMS and were not able to identify the ions they were detecting. Recently, Steiner, et al interfaced an atmospheric pressure ion mobility spectrometer to a time of flight mass spectrometer.²² This ion mobility time of flight mass spectrometer (IMtofMS) permitted the two dimension analysis of samples based on ion mobility and mass. Because ion mobility spectrometry separates ions based on their size to charge ratio, isobaric compounds can be separated prior to the introduction into the mass spectrometer. In addition, random noise, both chemical and electronic, is separated in mobility space, increasing the signal/noise ratio in the mass spectrum.

In this work, we use the IMtofMS to identify the response ions which inorganic anions produce when they are electrosprayed from aqueous solutions into an ion mobility spectrometer and evaluate the two dimensional mobility/mass separations of these anion mixtures. In particular, this study focuses on anions of environmental interest such as; nitrate, nitrite, sulfate, phosphate, arsenate, and arsenite.

EXPERIMENTAL

a) Instrumentation

The IM(tof)MS instrument used in this study was constructed at Washington State University in Pullman, Washington, USA. The major components of this instrument were an electrospray ionization source, an atmospheric pressure ion mobility tube, a vacuum interface, a time-of-flight mass spectrometer and data acquisition system. These components and the instrument's modes

of operation have all been described in detail elsewhere²⁰⁻²³. As such, only a brief description of the instrument follows.

Ions were generated via an electrospray source, consisting of a KD Scientific (New Hope, PA, USA) 210 syringe pump which maintained a 1 $\mu\text{l}/\text{min}$ flow rate through the 50.0 micron internal diameter (i.d.) capillary. Samples were dissolved in ESI solvent (90% methanol:10% water) solutions. A negative 13.3 kV potential was applied to the solution in the electrospray capillary via a metal union approximately 15 cm from the capillary tip. The capillary tip was placed slightly inside the target screen where maximum ion transmission was achieved. Electrosprayed droplets then traveled 8.0 cm through the ion mobility tube desolvation region, where sample ions traveled against a countercurrent 1.0 L/min flow of nitrogen at 250° C, facilitating desolvation of the drops to produce individual unclustered background or analyte ions.

The ion mobility tube used in these experiments employed a stacked ring design which has been explained in detail previously²⁴. It consisted of electrically conducting stainless steel “guard” rings and electrically insulating alumina rings. These guard rings were connected via a series of resistors (1.0 M Ω drift region and 0.5M Ω desolvation region), resulting in an electric field of 441 V/cm, in the 18.0 cm drift region, via a gate voltage of 7.94 kV. The ion gate was a Bradbury-Nielson type geometry and separated the desolvation region of the spectrometer from the ion drift region. Ion packets were introduced into the drift region from the desolvation region through the ion gate via 200 μs pulses at a frequency of 25Hz. In the drift region of the IMS, ions separated according to their size to charge ratio with the ions of higher velocities arriving at

the entrance to the mass spectrometer first. Ion velocities are inversely proportional to the ion's size to charge ratio.

After separation, ions traveled through an atmospheric pressure/vacuum interface where they migrated from 688-701 torr down to 1.7 torr. Pumping was achieved using a Varian DS602 rotary vane pump pumping at 600 L/min. A focusing lens in the interface allowed for adjustment of the collisional energy of the ions with residual gas particles. Consequently, collision induced dissociation (CID) was possible in the interface. Precursor ions and/or fragment ions created in the interface were injected into an orthogonal time-of-flight mass spectrometer which has been described previously.²⁵

From the IMS/MS interface, a series of ion lenses focused the ions into a parallel beam where they entered the extraction region of the mass spectrometer and were pulsed with -2.00 kV at a frequency of 50 kHz and a pulse width of 1.0 μ s into the drift region of the mass spectrometer. In this region, the pressure was maintained at roughly 2×10^{-4} torr by a 46L/s V70 turbo pump (Varian, Lexington, MA, USA)

Since the time spent in the TOF analyzer was negligible when compared to the time spent in the ion mobility analyzer the data acquisition software could record both an ion mobility drift time and a mass spectrometer drift time for each MCP event. Data acquisition and timing control, of the AP-IMS gate and TOFMS extractor, were achieved through the use of IonWerks²⁶ TOFMS time-to-digital converter and a dual Pentium III workstation running IonWerks 3D acquisition software. Data processing was further completed using Research Systems IDL virtual machine

6.0 software²⁷. Operating conditions for all experiments were as reported in Table 1 unless specified as otherwise.

b) Chemicals

The chemical standards used in this study were sodium nitrate (NaNO₃) and sodium meta-arsenite (NaAsO₂) purchased from Sigma-Aldrich; sodium nitrite (NaNO₂) from Fisher; sodium sulfate (NaSO₄), sodium hydrogen phosphate (NaH₂PO₄) and sodium chloride from J.T. Baker, and sodium hydrogen arsenate heptahydrate (NaHAsO₄ * 7H₂O) from Mallinckrodt Chemical Works. The ESI solvents used were HPLC grade methanol, purchased from J.T. Baker, and water. Aqueous storm water runoff samples were collected in the greater Seattle, WA, USA area; specifically out of Swamp Creek and runoff on Washington Street.

c) Calculations

Reduced mobility constants (K_o) were calculated using the following equation²⁴:

$$(1) \quad K_o = \frac{L^2}{t_d V} \left[\frac{273}{T} \right] \left[\frac{P}{760} \right]$$

where L is the length of the drift region (18 cm), t_d is the experimentally determined drift time of the ion (s), V is the voltage drop across the IMS drift region (7.94 kV), T is the temperature in the drift tube (523 K) and P is atmospheric pressure (688 – 701 torr). The resulting units for K_o being cm²/ (V*s).

RESULTS AND DISCUSSION

The spectra presented in this work plot the one dimensional mass data on the x-axis in units of mass to charge ratio versus the one dimensional ion mobility drift time data on the y-axis in units of microseconds. The result is a two dimensional plot where intensity is depicted by shading of the points located at the proper mass and mobility for the individual ions observed in the spectrum. Figure 1 shows examples of these two-dimensional mobility-mass spectra for sodium arsenate (A) and sodium arsenite (B). In all cases in this study, only the anions were investigated by operating the IMtofMS in the negative ion mode. The counter ions, sodium in this case, were never observed in the spectra.

In Figure 1A the mass spectrum of the 50 ppm sodium arsenate (NaH_2AsO_4) standard showed a small molecular ion peak as expected at $m/z = 141$ for the H_2AsO_4^- ion and a major ion peak at m/z of 123 resulting from the loss of water to produce the AsO_3^- ion. In the mobility spectrum, however, two major peaks were observed at drift times of 9.70 ms and 10.33 ms. The reduced mobility values (K_0) that were calculated from these drift times were $1.83 \text{ cm}^2/\text{V}\cdot\text{s}$ and $1.73 \text{ cm}^2/\text{V}\cdot\text{s}$, respectively. From the two dimensional spectrum, it was possible to determine a mass spectrum for each peak in the mobility spectrum. . The mobility selected mass spectrum for the slow mobility ion ($t_a = 10.33\text{ms}$, $K_0 = 1.73 \text{ cm}^2/\text{V}\cdot\text{s}$) contained a major peak at $m/z = 123$ corresponding to the AsO_3^- ion. The mobility selected mass spectrum for the faster mobility ion ($t_a = 9.70 \text{ ms}$, $K_0 = 1.83 \text{ cm}^2/\text{V}\cdot\text{s}$) contained two peaks at m/z values of 123 and 141 corresponding to the AsO_3^- and H_2AsO_4^- ions. Throughout the two-dimensional spectrum, other unidentified low intensity ions were observed. These can be attributed to the background

ionization or small amounts of contaminants in the electrospray solvent or sample. Here we focus on the major ions observed in the mobility and mass spectra

One explanation for the results obtained in Figure 1A is that the ion with a reduced mobility of $1.83 \text{ cm}^2/\text{V}\cdot\text{s}$ ($t_a = 9.70 \text{ ms}$) traveled through the mobility tube as H_2AsO_4^- and fragmented to the AsO_3^- ion at the IMS-MS interface. Because the ion of lower mobility produced only a AsO_3^- ion in the mobility selected mass spectrum and we know that the larger H_2AsO_4^- ion traveled faster than this ion, we assume that the ion with a reduced mobility of $1.73 \text{ cm}^2/\text{V}\cdot\text{s}$ ($t_a = 10.33\text{ms}$) traveled as the dimer ion $\text{H}_5\text{As}_2\text{O}_8^-$ which fragmented completely at the IMS-MS interface with a loss of water to form the AsO_3^- ion and the neutral acid H_3AsO_4 .

The ion mobility mass spectrum for 50 ppm solution of sodium arsenite (NaAsO_2) shown in Figure 1B was even more complex than that of the sodium arsenate. The mass spectrum produced major ions at $m/z = 107, 123, 141, 169, 215, 231, 247,$ and 305 which corresponded to AsO_2^- , AsO_3^- , H_2AsO_4^- . Figure 1B shows the metaarsenite solution; note the presence of many mobility/mass peaks. It was apparent in this spectrum that arsenate was present in the arsenite solution – in fact three different arsenic containing anions were detected in this experiment, hydrogen arsenate (H_2AsO_4^-), metaarsenate (AsO_3^-) and metaarsenite (AsO_2^-). In an effort to achieve a higher degree of sensitivity for the multiple peaks, the spectrum shown in Figure 1 was collected for 30 minutes. This spectrum shows examples where mobility was unable to resolve some peaks that could be resolved in the mobility-mass space of the 2-D separation. For example, the broad mobility peak at $\sim 9 \text{ ms}$ was possibly the result of three overlapping mobility peaks, two corresponding to metaarsenite peaks at 107 Da and one peak at 97 Da . The 97 Da

peak is most probably the result of sulfate contamination in the HPLC grade methanol being used in this study, not a fragment of the metaarsenite peak at 107 Da. This sulfate contaminant was present in the background, which was run just prior to this experiment. It had a drift time of 9.22 ms, which was included in the mobility range, 8.69 – 9.33 of the broad mobility peak seen in this spectrum.

Similarly, it was evident that individual mass peaks in the one dimensional mass spectra were actually the result of contributions from different chemical species. As mentioned it's possible that the 107 Da peak is in actuality two overlapping mobility peaks, as the two dimensional plot appears to have two maxima within the 107Da/~9 ms peak.

Also present was an arsenate peak at reduced mobility $1.84 \text{ cm}^2/\text{V}^*\text{s}$ with mass values of 141 Da and 123 Da. Note the close reduced mobility agreement with the corresponding peak ($1.83 \text{ cm}^2/\text{Vs}$) in Figure 1A. Also note the small shoulder on the $1.84 \text{ cm}^2/\text{Vs}$ peak. This peak had a mass/charge ratio of 89 Da and was present in the background.

The peak with a reduced mobility value of $1.71 \text{ cm}^2/\text{V}^*\text{s}$ was again the result of two overlapping mobility peaks. The first was that of the metaarsenate with a mass of 123 Da. The second was the 107 Da fragment ion from the 215 Da/ peak. The parent ion appeared to be a complex of two metaarsenite ions and a hydrogen, where the fragment peak corresponded to the loss of a neutral hydrogen metaarsenite. The overlap of two peaks explains why this peak has slightly different reduced mobility than the corresponding peak in Figure 1A. Isolation of the 123 Da peak in the

two dimensional spectrum allowed for a more accurate determination of its drift time (10.41 ms), resulting in a reduced mobility of $1.73 \text{ cm}^2/\text{V}\cdot\text{s}$ – exactly matching that found in Figure 1A.

The peak at a reduced mobility of $1.64 \text{ cm}^2/\text{V}\cdot\text{s}$ was also the result of two somewhat overlapping mobility peaks. The first corresponded to a series of masses, 231, 169, 123, 107 Da. It was identified as a metaarsenite/metaarsenate complex ($\text{AsO}_2^- \cdot \text{HAsO}_3^-$), where fragmentation at the vacuum interface resulted in individual metaarsenite and metaarsenate peaks, 107 and 123 Da respectively. The 169 fragment peak was unidentified. Isolation of this series of peaks in the two dimensional graph filters out the effects of the overlapping peak and allows for determination of the drift time for just this series of peaks – 11.0 ms resulting in a calculated reduced mobility of $1.64 \text{ cm}^2/\text{V}\cdot\text{s}$. The other distinct peak apparent in the two dimensional spectra but with overlapping mobility in the one dimensional mobility spectra had a mass of 247 Da with no fragments. This peak was a complex of two metaarsenate anions and a hydrogen, isolation of this peak in the two dimensional spectra results in a drift time of 10.41 ms and a calculated reduced mobility of $1.62 \text{ cm}^2/\text{V}\cdot\text{s}$.

The final peak identified in this Figure 1B was again an arsenic containing complex with 3 arsenics in the 3+ oxidation state and 5 oxygens. These data show two distinct mobilities, although they do not exhibit baseline resolution, one with a drift time of 12.04 ms ($K_0 = 1.50 \text{ cm}^2/\text{V}\cdot\text{s}$) and the other with a drift time of 12.14 ms ($K_0 = 1.49 \text{ cm}^2/\text{V}\cdot\text{s}$). While mass analysis and sample composition support that these peaks were the result of three arsenics and 5 oxygens, the structure of this complex was unknown.

Figure 2 shows one of the primary advantages of ion mobility spectrometry when coupled to mass spectrometry – the differentiation of isobars. For example, hydrogen phosphate, in the H_2PO_4^- state, has a mass of 97 Da, as does the hydrogen sulfate anion, HSO_4^- . Figure 2A shows data resulting from electrospraying 50ppm of a hydrogen phosphate solution. Note the loss of a water to form a fragment ion at 79 Da. Figure 2B shows the spectrum from 50ppm sulfate solution. It is evident in this spectrum that sulfate does not show the loss of water that phosphate does. This fact could be used to differentiate between the two with just a mass spectrometer however, 97/79 peak intensity ratios must be used to determine the presence and relative amounts of sulfate and phosphate in a given sample. Mobility-mass spectrometry easily distinguishes between the phosphate and sulfate peaks, with almost baseline resolution, as is shown in Figure 2C. Because sulfate had a stronger electrospray ionization response than phosphate, the sulfate/phosphate mixture was 1:2, 25ppm sulfate and 50ppm phosphate in order to achieve similar peak intensities. The sulfate peak had a drift time of 9.18 ms yielding a reduced mobility of $1.97 \text{ cm}^2/\text{V}\cdot\text{s}$. This was comparable to figure 2B which showed sulfate with a drift time of 9.19 ms yielding a reduced mobility of $1.98 \text{ cm}^2/\text{V}\cdot\text{s}$. Because the experiments were conducted on the same day and under the same conditions, drift times can be directly compared. The difference in drift times for all sulfate ions measured was no more than 0.03 ms, whereas the average peak width was 0.34 ms. The phosphate peak, on the other hand, had the exact same reduced mobility value ($1.92 \text{ cm}^2/\text{V}\cdot\text{s}$) in the mixture spectrum as in the individual one and was clearly resolved from the sulfate peak in the mixture.

The power of tandem ion mobility/mass spectrometry lies in its ability to rapidly separate mixtures. Figure 3 shows a mixture of seven anions of interest. Note that since the sodium

metaarsenite solution showed both arsenate, arsenite and arsenate/arsenite complex peaks it alone was used as the source of arsenate and arsenite in the mixture data. Also note that different concentrations were used in an effort to equalize peak heights. The mixture was made as follows, 2.5ppm NO₃, 6.5ppm NO₂, 70ppm Arsenate/Arsenite, 9ppm Cl, 30ppm H₂PO₄, 15ppm HSO₄.

Figure 3A is the spectrum resulting from the above mixture run for 10 minutes with a 200 μs ion mobility gate pulse width – identical to all the previously discussed work. It is evident in this spectrum that there were at least 10 clearly resolved peaks corresponding to the aforementioned components. However, with a mixture like this greater resolving power was desired and consequently the trials were re-run with the gate pulse reduced to 100 μs, the gate voltage reduced to 7.99 kV and the acquisition time increased to 60 minutes. It is evident in this spectrum that there are at least 15 clearly resolved peaks. These 15 peaks are identified with letters A-O. Table 2 shows the drift time, reduced mobility, mass (parent then fragments), resolving power and identity of peaks A-O. It is of interest that peaks K-O are complexes of ions present in solution. For example, peak L is a complex of the hydrogen phosphate ion with a metaarsenite ion and an H⁺. While data wasn't presented specifically showing this fact, it was and has previously been noted that complexes of multiple anionic species were concentration dependent. At greater sample concentration some anions show dimer and trimerization. As such one anion of interest may be present in the IMS with multiple drift times due to dimers, trimers, etc... Peaks K-O demonstrate said dimerization and presumably upon variation of the concentrations in the mixture these dimer peaks could be made to come and go.

Note that four of these peaks are designated as background peaks as they were evident in the background spectrum taken prior to this experiment and under the same conditions. It is presumed that these peaks are present because the HPLC grade methanol was not cleaned before its use in these series of experiments. Possible identifications, based on mass and likely methanol contaminants, are suggested for some of the background peaks but these have not been confirmed through experimentation.

A desired outcome of this series of experiments was to show a potential for IMS as a detector for inorganic anionic contaminants in real world samples and to identify ions associated with the mobility spectra. Figure 4 shows IMMS spectra resulting from the analysis of storm water runoff samples collected in the Seattle, WA, specifically in swamp creek and on Michigan Street. These samples were stored in plastic containers at five degrees Celsius. Immediately prior to the experiment, samples were filtered through 25mm membrane filters and this filtered water was mixed with methanol at a ratio of 75% methanol to 25% filtered storm runoff water. Note that this ratio was not the same as the 90/10 ratio for previous trials in order to dilute the sample as little as possible while still having a solution compatible with negative mode electrospray. Also note that these experiments were done at the longer IMS gate pulse width thereby having lower resolving powers and that these spectra were averaged for 15 instead of 10 minutes.

Figure 4A shows a background spectrum taken just prior to and under the same conditions as the real samples 4B and 4C, where 4B is from swamp creek and 4C from Michigan Street. The previously mentioned background peaks are present in this spectrum as are chloride, nitrate, nitrite and sulfate peaks. Both the swamp creek and Michigan Street samples show increases in

chloride, nitrate, nitrite and sulfate peak intensities. Arsenate and arsenite peaks are present in the swamp creek sample. These peaks were not present in the background and are not present in the Michigan Street sample.

CONCLUSIONS

These series of experiment demonstrate the potential for the use of IMS as a stand alone instrument for the analysis of anionic mixtures in real world samples. Data from both the artificial mixture and real storm water runoff samples show separation of anions via IMS. When the gate pulse width is reduced to 100us, baseline resolution in the IMS spectrum is observed, even for a set of isobaric compounds (H_2PO_4 and HSO_4). However, the spectra are complicated and it is noted, specifically with the arsenic species, that one anionic species can be present as multiple IMMS peaks corresponding to anion complexes. It's presumed, based on previous laboratory experiences, that the presence, or lack thereof, of these ion complexes varies with the concentration of the analytes used. The effect of concentration on dimer and trimerization, and hence mobility peaks present in a sample should be an area of future study stemming from this work. Nevertheless, given the mass and reduced mobility identification of peaks in this work it seems reasonable that a stand alone IMS could be taken into the field and analysis of anions of interest conducted based solely on ion drift times. Depending on the composition of the sample mixture one may find it necessary to bring a sample back to the lab for more detailed IMMS analysis. Given the portable nature of IMS devices, it seems reasonable to conclude, that as a field instrument, IMS stands to yield rapid, field identification of anions in real world samples or

at least function as a good screening tool offering information with regards to which samples warrant further laboratory workup and which do not.

In addition to identifying the potential application of IMS to field analysis of anions, this is the first time tandem ion mobility mass spectrometry has been used to analyze inorganic anions. Anions were analyzed both individually, in a real world sample and synthetic mixtures. The power of IMS lies in its ability to separate different components with the same mass based on their size to charge ratio. This was demonstrated with sulfate and phosphate and also where the fragment of the hydrogen arsenate ion, metaarsenate, overlapped with the metaarsenate ion signal in the one dimensional mass spectra. The tandem nature of IMMS enables the separation of ions that do not exhibit baseline resolution in a one dimensional mobility spectrum. The two attributes combined allow the analysis of complicated mixtures that could not be done with either instrument alone.

ACKNOWLEDGEMENTS

The authors acknowledge dTech, Seattle, WA for partial support of this work through an SBIR grant from the Environmental Protection Agency.

REFERENCES

1. Peyton, B.M.; Peterson, J.N. *Water Res.* **2001**, 35, 215-231.
2. Weisburger, J.H. *Nutr. Cancer*, **1986**, 8, 47-62.
3. Carson, T.L. *Vet. Clin. North. Am. Food. Anim. Pract.*, **2000**, 16, 455-464.
4. Connolly, D. *Anal. Chim. Acta*, **2001**, 441, 53-62.
5. W.H.O. *Tech. Rep. Ser.*, **1995**, 859, 1-54.
6. Oldreive, C.; Rice-Evans, C. *Free Radical Res.*, **2001**, 35, 215-231.
7. Graham, E. *Clin. Biochem* **1998**, 31, 195-220.
8. Abernathy, C.O.; Liu, Y.; Longfellow, D.; Aposhian, H.V.; Beck, B.; Fowler, B.; Goyer, R.; Menzer, R.; Rossman, T.; Thompson, C.; Waalkes, M. *Env. Health Pers.* **1999**, 107(7), 593-597.
9. Greenberg, A.E.; Clesceri, L.S.; Eaton, M.A. *American Public Health Association*, 18th edition, **1992**, 1-4.
10. Office of Ground Water and Drinking Water Standards and Risk Management Division, U.S. EPA, EPA-815-R-00-010, **1999**
11. Forte, G.; Amato, D.; Caroli, S. *Microchem. Journal*, **2005**, 15-19.
12. Florencio, M.H.; Duarte, M.F.; Bettencourt, A.M.M.; Bomes, M.L.; Vilas Boas, L.F. *Rapid Comm. in Mass Spec.* **1997**, 11, 469-473.
13. Schramel, O.; Michalke, B.; Kettrup, A. *J. Anal. At. Spec.* **1999**, 14, 1339-1342.
14. McSheehy, S.; Szpunar, J.; Lobinski, R.; Haldys, V.; Tortajada, J.; Edmonds, J.S. *Anal. Chem.* **2002**, 74, 2370-2378.
15. Shumate, C.B.; Hill, H.H. *Anal. Chem.* **1989**, 61, 601-606.
16. Wittmer, D.; Luckenbill, B.K.; Chen, Y.H.; Hill, H.H. *Anal. Chem.* **1994** 66, 2348 – 2355.
17. Dion, H.M.; Ackerman, L.K.; Hill, H.H. *Talanta*, **2002**, 57, 1161-1171.
18. Dwivedi, P.; Matz, L.M.; Atkinson, D.A.; Hill, H.H. *Analyst* **2004**, 129, 139-144.
19. Eiceman, G.A. *Crit. Rev. Anal. Chem.* **1991**, 22, 17-36.
20. Steiner, W.E.; Clowers, B.H.; Matz, L.M.; Siems, W.F.; Hill, H.H., *Anal. Chem.*, **2002**, 74, 4343- 4352.
21. Steiner, W.E.; Clowers, B.H.; Haigh, P.E.; Hill, H.H., *Anal. Chem.*, **2003**, 75, 6068-6076.
22. Steiner W.E.; Clowers B.H.; Fuhrer K.; Gonin M.; Matz L.M.; Siems W.F.; Schultz A.J.; Hill H.H., *Rapid Comm Mass Spectrom*, **2001**, 15, 2221.
23. Matz, L.M.; Steiner, W.E.; Clowers, B.H.; Hill, H.H. *International J. Mass Spec.* **2002**, 213, 191-202.
24. Wu, C.; Siems, W.F.; Asbury, G.R.; Hill, H.H., *Anal. Chem.* **1998**, 70, 4929-4938.
25. Gonin, M.; Fuhrer, K.; Schultz, A.J., *12th Sanibel Conference on Mass Spectrometry*, Field Portable and Miniature Mass Spectrometry, 2000.
26. Ionwerks 3-D, *Ionwerks Inc*, Houston TX, **2004**.
27. Transform V3.4, *Fortner Software LLC*, Serling VA, **1998**. Research Systems IDL virtual machine 6.0, *Research Systems Inc.*, Boulder CO, **2004**.

CAPTIONS

Table 1: IMtofMS Operating Conditions Summary

Table 2: Figure 3 (Anion Mixture) Peak Identities

Figure 1: A and B are 2D spectra of arsenic samples. A is 50ppm sodium arsenate solution, B is 50ppm sodium metaarsenite solution. Spectrum A shows the hydrogen arsenate ion ($\text{H}_2\text{AsO}_4^{-1}$ – 141 Da) and its fragment ion metaarsenate (AsO_3^{-}), corresponding to the loss of water. The metaarsenate ion is also present in solution, not as a fragment. Spectrum B, to which arsenate was not added, likewise shows these peaks. In addition, peaks corresponding to metaarsenite (AsO_2^{-}) and various arsenite/arsenate complexes are apparent in spectrum B.

Figure 2 shows analysis of sulfate and phosphate. In these experiments sulfate is detected as HSO_4^{-} and phosphate as $\text{H}_2\text{PO}_4^{-}$, both of which have a mass of 97 Da. A shows sulfate data while B shows phosphate data. Note the presence of a 79 Da fragment ion, the result of a loss of water in spectrum A. Phosphate doesn't exhibit this loss of water. Spectrum C shows the separation of phosphate and sulfate via ion mobility – a distinction only possible by looking at the fragmentation pattern by MS alone.

Figure 3 shows a mixture of 2.5ppm NO_3 , 6.5ppm NO_2 , 70ppm Arsenate/Arsenite, 9ppm Cl, 30ppm H_2PO_4 and 15ppm HSO_4 . Note that only the metaarsenite sample was used as arsenate, arsenite and arsenate/arsenite complexes are present, as such a higher concentration is used. Unequal concentrations were an attempt to better equalize the resulting peak intensities. Spectrum A had the same experimental conditions as all previous experiments. Spectrum B better shows the resolving power potential of IMMS (around 100 for the mobility spectrum) by reducing the pulse width to 100us. However, the data acquisition time had to be increased to 60 minutes. Peaks A-O are identified in Table 2.

Figure 4 shows the results from real samples collected in the greater Seattle, WA, USA area. 4A is a background spectra, note the presence of nitrate, nitrite, chloride and sulfate in the background spectra. It was determined these were most probably due to contamination in the HPLC grade methanol. 4B shows a swamp creek sample and features corresponding to arsenate and arsenite are present in the spectrum. These results were not quantified. Figure 4C shows a sample collected on Washington Street, all features were present in the background, however, analytes of interest are present in the background. The analytes of interest in the Washington street sample seem to show increased intensities. Further work should be done with clean methanol.

Table 1: IMtofMS Operating Conditions Summary

| | |
|---|--|
| Electrospray Ionization | ESI Voltage = -13330 V ESI Sampling Rate = 1.0 μ L/min |
| Ion Mobility Spectrometer | Pressure = 688 - 701 Torr Temperature = 250 $^{\circ}$ C Target Screen Voltage = -9201 V Gate Voltage = 7940 V Drift Length = 18.0 cm Drift Gas Inlet Block Voltage (Shower Head) = 150.0 V Nitrogen Drift Gas Flow Rate = 1.0 L/min |
| Interface | Pressure = 1.4 Torr Nozzle Lens = -207 V Focus Lens = -171.2 V Skimmer Lens = -109.5 V |
| Time-of-Flight Mass Spectrometer | Pressure = 2.1×10^{-6} Torr Lens 1 = 7.4 V Lens 2 = 124.8 V Deflector Up Lens 3 = -9.5 V Deflector Down Lens 4 = 1.2 V Lens 3 = -23.2 V Reflector Back Plane = -679.9 V Reflector Grid Plane = 239.3 V Extraction Region Loading = 720.0 V Extraction Region Pulsing = -738.0 V Field Free Region = 2000.0 V MCP Bias = 2454.0 V |
| Acquisition Timing | TOFMS Resolution = 1.25 ns IMS Gate Pulse Frequency = 25.0 Hz IMS Gate Pulse Width = 200.0 μ s TOFMS Extraction Frequency = 50 kHz TOFMS Extraction Pulse Width = 1.0 μ s |
| Miscellaneous | Sampling = 10 min runs All Sampling Sets = 3 runs per data point |

| Table 2: Figure 3 (Anion Mixture) Peak Identities | | | | | |
|--|------------|------|-----------|------|--|
| | Drift (us) | Ko | Mass (Da) | RP | Parent Ion |
| A | 7201 | 2.71 | 35,37 | 63.4 | Cl ⁻ |
| B | 7758 | 2.52 | 46 | 79.5 | NO ₂ ⁻ |
| C | 8050 | 2.43 | 45 | 96.6 | BCK |
| D | 8365 | 2.33 | 60 | 92.2 | BCK |
| E | 8612 | 2.27 | 62 | 88.3 | NO ₃ ⁻ |
| F | 9033 | 2.16 | 60 | 93.3 | BCK |
| G | 9221 | 2.12 | 59 | | C ₂ H ₃ O ₂ ⁻ - BCK |
| H | 9863 | 1.98 | 97 | 96.4 | HSO ₄ ⁻ |
| I | 10163 | 1.92 | 97,75 | 135 | H ₂ PO ₄ ⁻ |
| J | 10569 | 1.83 | 141,123 | 112 | H ₂ AsO ₄ ⁻ |
| K | 11283 | 1.73 | 215,107 | 69.8 | (AsO ₂ ⁻) ₂ *H ⁺ |
| L | 11620 | 1.73 | 187,79 | 120 | HPO ₃ *AsO ₂ ⁻ *H ⁺ |
| M | 11841 | 1.65 | 231,123 | 42.8 | AsO ₃ ⁻ *AsO ₂ ⁻ *H ⁺ |
| N | 12029 | 1.62 | 247 | | (AsO ₃ ⁻) ₂ *H ⁺ |
| O | 13015 | 1.5 | 305 | 110 | As ₃ O ₅ ⁻ |

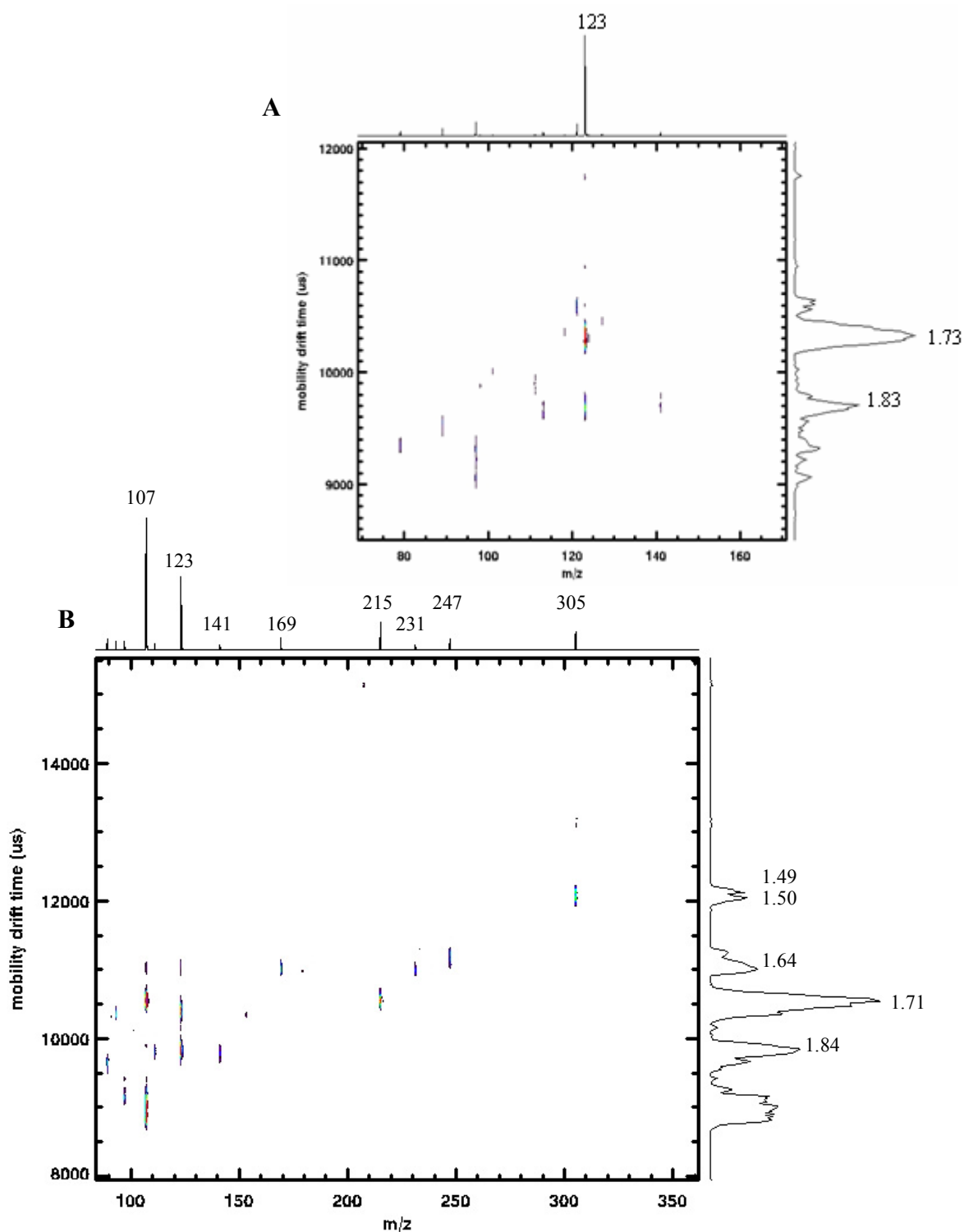


Figure 1: A and B are 2D spectra of arsenic samples. A is 50ppm sodium arsenate solution, B is 50ppm sodium metaarsenite solution. Spectrum A shows the hydrogen arsenate ion ($\text{H}_2\text{AsO}_4^{-1}$ – 141 Da) and its fragment ion metaarsenate (AsO_3^-), corresponding to the loss of water. The metaarsenate ion is also present in solution, not as a fragment. Spectrum B, to which arsenate was not added, likewise shows these peaks. In addition, peaks corresponding to metaarsenite (AsO_2^-) and various arsenite/arsenate complexes are apparent in spectrum B.

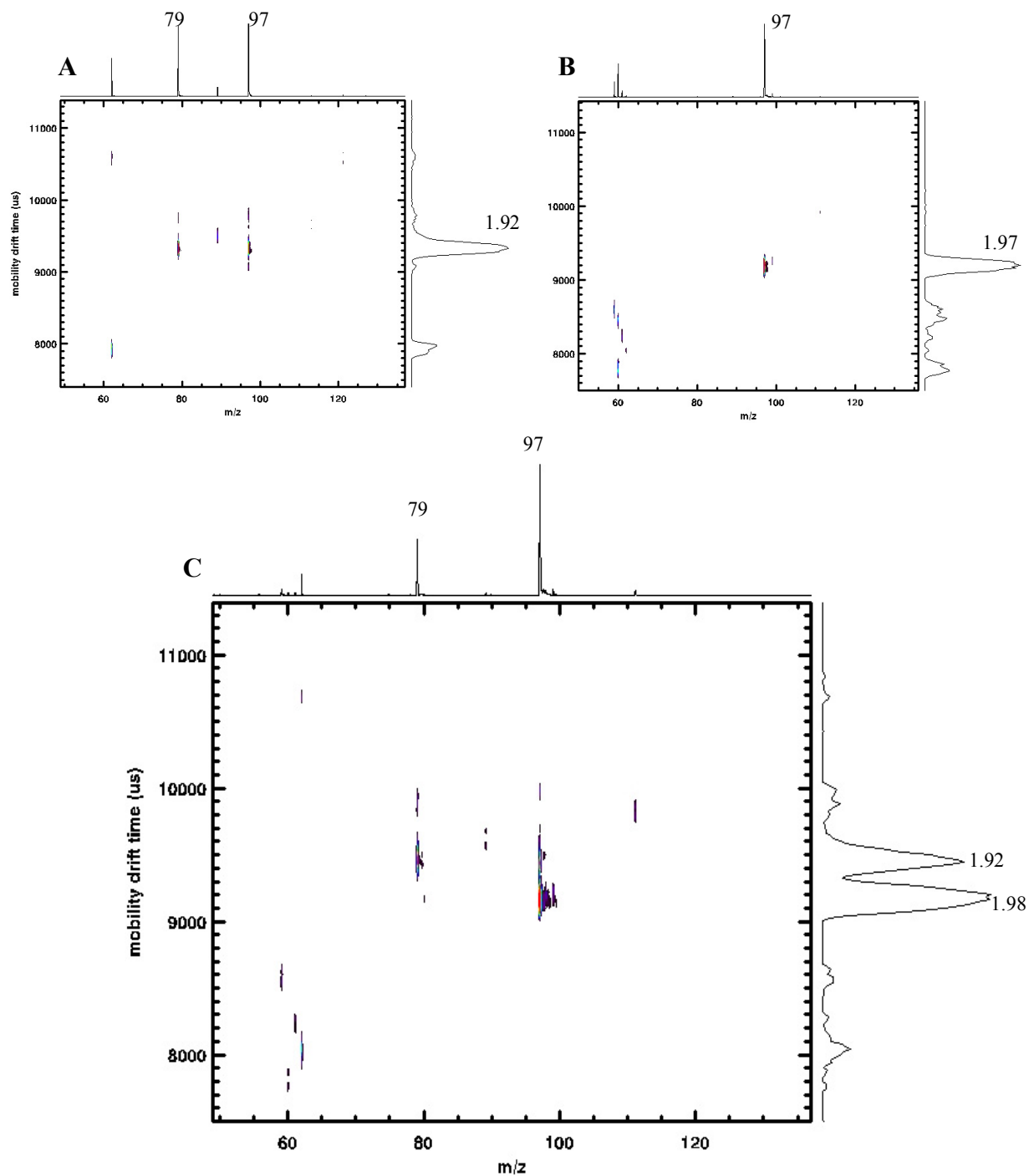


Figure 2 shows analysis of sulfate and phosphate. In these experiments sulfate is detected as HSO_4^- and phosphate as H_2PO_4^- , both of which have a mass of 97 Da. A shows phosphate data while B shows sulfate data. Note the presence of a 79 Da fragment ion, the result of a loss of water in spectrum A. Spectrum C shows the separation of phosphate and sulfate via ion mobility – a distinction only possible by looking at the fragmentation pattern by MS alone.

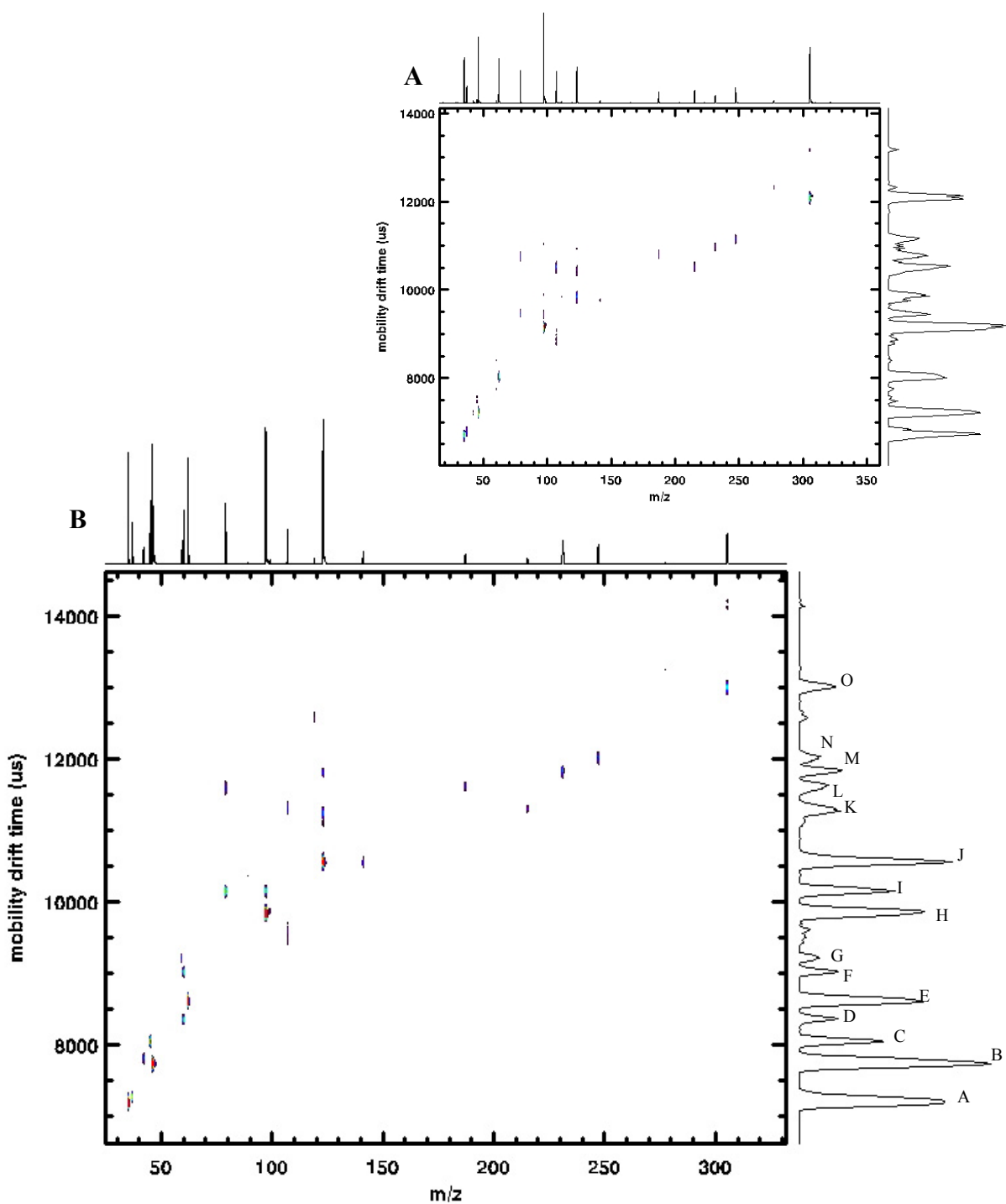


Figure 3 shows a mixture of 2.5ppm NO_3^- , 6.5ppm NO_2^- , 70ppm Arsenate/Arsenite, 9ppm Cl^- , 30ppm H_2PO_4^- and 15ppm HSO_4^- . Note that only the metaarsenite sample was used as arsenate, arsenite and arsenate/arsenite complexes are present, as such a higher concentration is used. Unequal concentrations were an attempt to better equalize the resulting peak intensities. Spectrum A had the same experimental conditions as all previous experiments. Spectrum B better shows the resolving power potential of IMMS (around 100 for the mobility spectrum) by reducing the pulse width to 100us. However, the data acquisition time had to be increased to 60 minutes. Peaks A-O are identified in Table 2.

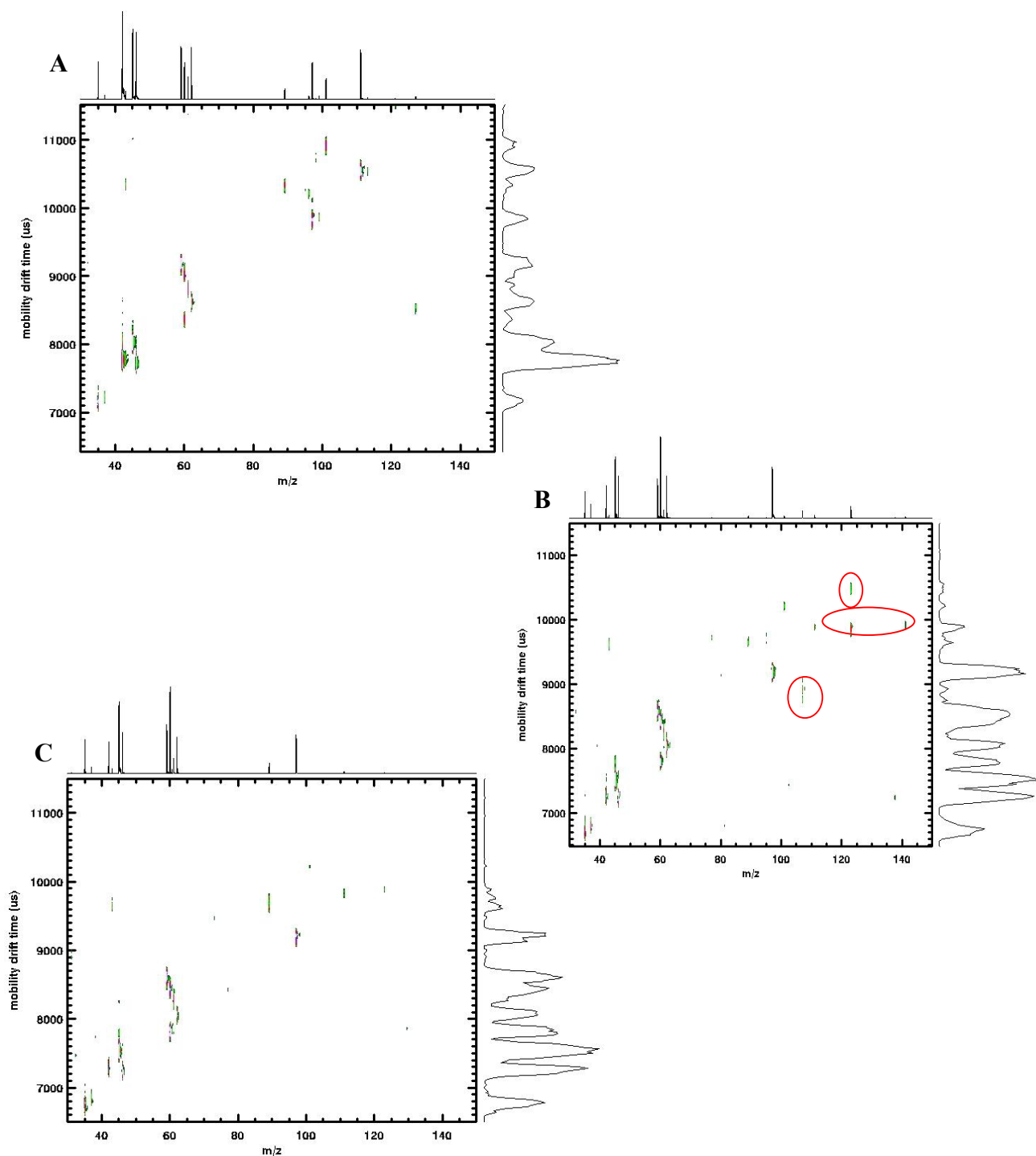


Figure 4 shows the results from real samples collected in the greater Seattle, WA, USA area. 4A is a background spectra, note the presence of nitrate, nitrite, chloride and sulfate in the background spectra. It was determined these were most probably due to contamination in the HPLC grade methanol. 4B shows a swamp creek sample and features corresponding to arsenate and arsenite are present in the spectrum. These results were not quantified. Figure 4C shows a sample collected on Washington Street, all features were present in the background, however, analytes of interest are present in the background. The analytes of interest in the Washington street sample seem to show increased intensities. Further work should be done with clean methanol.

CHAPTER 3

Separation and Detection of a Protein Mixture using Ion Mobility Time-of-Flight Mass Spectrometry

By

Steven J. Klopsch, Wes E. Steiner and Herbert H. Hill*.

Department of Chemistry

Washington State University

Pullman, WA 99164-4630

Tel: (509) 335-5648

Fax: (509) 335-8867

E-mail: hhill@wsu.edu

**To be Submitted to
Analytical Chemistry**

*** to whom correspondence should be addressed**

ABSTRACT

The detection and identification of intact proteins is of great interest – specifically detection of intact proteins in a complex mixture. The field of proteomics requires separation and identification of proteins in a complex biological matrix. Detection of biotoxins in the environment would likewise require analysis of complex mixtures. Ion mobility spectrometry and FAIMS coupled with mass spectrometry have been applied to the detection of peptides in complex mixtures and individual intact proteins. However, little work has been done with IMMS as it applies to the separation and detection of protein mixtures – prior to CID or digestion. This work employs an atmospheric pressure IMtofMS instrument for the analysis of various intact proteins followed by a mixture of those proteins. It is noted that the various protein charge states fall on certain size to mass trend lines. These trend lines are protein specific and can be used to identify which charge state peaks correspond to which proteins in protein mixtures.

INTRODUCTION

a) Individual Proteins

The use of ion mobility spectrometry for the detection of proteins and their specific charge states was first demonstrated by Wittmer, et al. in 1994.^{1,2} This research focused on the implementation and improvement of electrospray ionization as the ionization source for ion mobility spectrometry. As such, the focus was specifically on improvements to data acquisition as a result of changes to the electrospray configuration. Nonetheless it's the first example of identification of multiple protein (Cytochrome c) charge states via IMS, however, baseline resolution was not observed for these species.

Cytochrome c has since been widely used in IMS and IMMS experiments, including but not limited to analysis by High-Field Asymmetric Waveform IMS (FAIMS),^{3,4} IMS,^{1,5,6} IM-QMS,⁷⁻¹⁰ IMtofMS,¹¹⁻¹² FAIMS-IMtofMS⁴ and Hadamard Transform IMS.¹³ Investigating Cytochrome c has been the study of some of these works with goals including probing gas phase conformations of charge states and monitoring ion structural changes throughout the course of the experiment. In other experiments Cytochrome c was just a well documented molecule of choice used for improving ion mobility technique and verifying effectiveness of new instruments.

The first baseline resolution ion mobility spectra of a proteins' multiple charges states (Cytochrome c and Ubiquitin) were presented by Hill, *et al.* in 1998 on an AP-IM-QMS.¹⁰ Atmospheric pressure ion mobility spectrometry was shown in this work to have resolving powers high enough to justify IMS as a separations technique in its own right, providing

orthogonal separations data justifying a tandem IMMS instrument where ion mobilities are the means of separation. Also in 1998, the first IMtofMS data of biomolecules was reported,¹⁴ demonstrating simultaneous collection of both ion mobility and mass spectrometry data. The simultaneous analysis in two dimensions provided increased resolution. Data collected for the Ubiquitin protein showed baseline resolution in the mass domain while at the same time demonstrating the existence of multiple conformations, for certain m/z values, due to the added width, and/or bimodal distribution in the mobility domain.

Further IMMS work with individual proteins has been performed using FAIMS-MS.^{3,4,15-18} FAIMS is an atmospheric pressure ion mobility technique that separates ions based on their differing mobilities in high and low electric fields. It has found its primary application in protein analysis as a filtering device prior to MS. Similar to IM-QMS instruments mass and mobility data cannot be collected simultaneously. ESI-FAIMS-MS and ESI-FAIMS-MS/MS experiments have been performed in order to demonstrate the usefulness of FAIMS as a filtering device making analysis of mass spectra easier for Cytochrome c¹⁵, and Ubiquitin.¹⁶⁻¹⁸ Furthermore, in the case of Ubiquitin, gas phase conformers for various charge states were studied in detail. While the FAIMS device led to much simpler mass analysis and the ability to differentiate between conformers in the mobility domain in most cases baseline resolution was not evident in the mobility spectra. Similar analysis of gas phase Cytochrome c conformers has been conducted by Clemmer *et al.* employing the use of an ion trap-IM-QMS.^{6,10} Specifically this work looked at the folding and unfolding of ions throughout the duration of the experiment. The longer the ions spent in the trap, prior to IM-QMS analysis the more different conformers of the same charge state were detected.

b) Protein Digests and CID Analysis

IMMS work, as it relates to proteins, has also focused on MS/MS protein fragmentation experiments and protein digests. The use of IMS to separate the resulting peptides has proved to be very useful and there are many, many examples of said work in the literature. However, the novel work being reported here focuses on the use of ESI-IMS to separate mixtures of intact proteins. As such, a select few examples of separations of peptide mixtures, via protein digest or CID, are included here in an effort to recognize this important on going work in a related field of study.

Separations of peptide mixtures resulting from protein digests or CID of whole proteins have been demonstrated in several experiments. These include ion trap-MS/MS-IMtofMS analysis of Ubiquitin and Insulin;¹⁹⁻²¹ Nano-LC-IMtofMS analysis of *Drosophila* protein extract digest;²² Nano-LC-IM-CID-tofMS analysis of digested, soluble human urine proteins;²³ ESI-FAIMS-MS analysis of a pig hemoglobin tryptic digest;²⁴ Nano-LC-ESI-FAIMS-MS of rat plasma samples;²⁵ and IMS-IMS or IMS-IMS-IMS/MS of peptide and protein fragments.²⁶⁻²⁸ In all the sources above employing the use of Nano-LC the primary peptide separations step is the LC, the IMS is primarily separating different charge state conformations.

Clemmer's insulin and ubiquitin work¹⁹⁻²¹ are presented in greater detail here because they exhibit two different approaches to peptide analysis of proteins that have undergone CID using IMMS. The first strategy involves IMS analysis prior to CID²⁰ while the second involves IMS analysis of the fragments after CID.^{19,21} In the IMS before CID experiment ions were

accumulated in an ion trap, injected into an IMS, mass selected in a QMS, fragmented in an octopole collision cell and then the fragments were analyzed via TOF-MS. It's important to note in this experiment that while mobilities are being determined for the whole protein prior to CID the QMS not the IMS was the separations step prior to fragmentation and mass analysis. Nonetheless since IMS and TOF-MS happen on such different time scales two-dimensional mobility and mass data were collected for the fragments and fragments identified as belonging to which conformers. Fragmentation pattern similarities and differences were then analyzed for two different gas phase conformations of the same ubiquitin charge state.

The second instrumental approach to protein CID analysis involves mass selection and fragmentation of a protein charge state prior to determination of ion mobilities. As such, in these experiments the ion mobility was being used to help separate peptide fragment ions prior to TOF-MS, intact proteins never entered the drift region of the instrument. The result was the identification of charge state families where protein fragments with the same charge state fell on identifiable trend lines within the m/z vs. drift time data.

Most recently Clemmer, *et al.*²⁶⁻²⁸ used IMS-IMS and IMS-IMS-IMS/MS to analyze tryptic peptide mixtures and insulin chain B/ubiquitin fragments. This was similar to the work completed here in that IMS acts as a primary separations step for intact proteins – namely insulin chain B and ubiquitin prior to further analysis. They also have analyzed a mixture of peptides using IMS as the primary separations step for the peptides prior to a second IMS analysis of a selected charge states fragment ions.

c) Protein Mixtures

The purpose of this research was to investigate the potential of ESI-IMS as the separations technique for mixtures of proteins. Very little work has been done with the separation of intact proteins in a mixture using IMS. Clemmer, *et al.* have analyzed protein mixtures using a nano-LC/IMS-MS instrument.²⁹ However, the primary means of protein separation in these experiments is the nano-LC. Proteins that have already been separated using the LC are then analyzed using the IMS-tof-MS. Smith *et al.* used FAIMS and IMS in tandem as a separations technique then analyzed using time of flight mass spectrometry.³⁰ A sample of thirty peptides and proteins was prepared and analyzed. Sixteen FAIMS compensation voltages were selected and used as ion filters. IMMS spectra were then collected for each of the 16 CV's. IMMS spectral complexity was markedly decreased through the use of FAIMS as a filter, leading to easier identification of peaks in the 2D IMMS spectra.

This work used IMS as the sole separations device prior to TOF-MS, for the analysis of individual proteins and a synthetic protein mixture. The detection of individual proteins was presented in an effort to identify size to charge vs. mass to charge trend lines specific to individual proteins. This group was also interested in the capabilities of stand-alone IMS as a portable monitoring tool for biotoxins. The proteins selected in this work were representative, in terms of the mass range they covered, of typical biotoxins one might find naturally or maliciously in the environment. The degree to which IMS alone was able to separate protein charge states and/or proteins in a mixture would provide information towards the viability of the use of IMS a stand alone detector. In addition mass identification of charge states and determination of K_0 values could lead to definitive identification of the identity of an analyte

based solely on its mobility detected in a stand alone IMS unit. Finally, an instruments usefulness for monitoring real samples requires its ability to differentiate between multiple species in a mixture, to this end a mixture of proteins was analyzed for the degree of separation detected in the mobility domain. Furthermore the possibility of using charge state trend lines to identify which peaks belong to which proteins in a 2D spectrum was investigated.

EXPERIMENTAL

a) Chemicals, solvents and samples

Chemicals studied in this series of experiments were proteins ordered from the Sigma-Aldrich Chemical Company (St. Louis, MO, USA). They included Insulin purified from porcine pancreas tissue (I5523), insulin purified from bovine pancreas (I5500), a lyophilized powder of aprotinin from bovine lung tissue (A1153), lyophilized powder of lysozyme extracted from chicken egg white (L7651) and cytochrome c extracted from chicken heart (C0761). HPLC grade solvents used were water, methanol and acetic acid purchased from J.T. Baker (Phillipsburg, NJ, USA). Solutions of all the above protein samples were made at 100 or 200 μM in positive mode electrospray solvent - 47.5% water, 47.5% methanol and 5% acetic acid (v/v).

b) Instrumentation

The instrument used in this study was an atmospheric pressure – ion mobility – time of flight mass spectrometer constructed at Washington State University – previously described in detail.³¹⁻

³⁴ As such, only those details specific to this experiment will be discussed herein. Ions were

generated using an electrospray source consisting of a KD Scientific 210 syringe pump (New Hope, PA, USA). Sample solution traveled to the front of the IMS tube via a 50 micron i.d. capillary at a rate of 5 $\mu\text{L}/\text{min}$. Approximately 15 cm before the front of the IMS tube the solution traveled through a metal union where a potential of positive 13.3 kV was transferred to the solution. This is an approximate measurement because smooth operation of the electrospray device required consistently removing small sections from the tip of the capillary as it became clogged. The front of the IMS tube was capped with a target screen. The electrospray capillary extended from outside the IMS target screen, through the screen and terminated immediately inside the IMS tube. The actual distance the capillary extended into the IMS tube was not measured but rather placed in a location yielding maximum ion transmission. Electrosprayed droplets traveled 8.0cm within the ion mobility tube before reaching a Bradbury-Nielson style ion gate. This 8.0cm region served to desolvate ions as they traveled against a 1L/min counter-current flow of 200 or 250°C (depending on the experiment) nitrogen gas. Ions were guided through this desolvation portion of the tube and further through the drift portion, on an electric field established by a series of stacked insulating alumina and conducting stainless steel rings. In the desolvation region steel rings were connected with 0.5M Ω resistors and by 1.0 M Ω resistors in the drift region. The result was an applied field strength of 406.7 V/cm in the 18.0 cm drift region, as the voltage dropped from 7.94 kV at the ion gate to 170 V at the interface to the tof-MS. Ions were pulsed through the gate, with a pulse width of 500 μs at a frequency of 30 times per second. Ion packets were then separated based on their size to charge ratio.

After separation, ions entered the tof-MS through an atmospheric pressure/vacuum interface where they migrated from 698-701 torr down to 1.7 torr. Focusing lens voltages were adjusted

to minimize collisionally induced dissociation but this also significantly reduced ion transmission. The nozzle voltage was set at 169.4 V, focusing at 170V and the skimmer voltage at 99.2V. Note the nozzle voltage, the one closest to the ion mobility tube, is less than the focusing voltage. All work with smaller analytes of interest on this instrument has been done with steadily decreasing voltages, guiding the ions down the field gradient until entering the tof-MS. Ions with molecular weights in the thousands are only detectable on this instrument when there is a very slight increase in voltage within the interface, as shown above. This arrangement of voltages ultimately results in decreased ion transmission.

After the interface, ions traveled through another series of lenses before entering the tof extraction region where the pressure was held at roughly 2×10^{-4} torr by a 46L/s V70 turbo pump (Varian, Lexington, MA, USA). This second set of lenses arranged the ions into a parallel beam for extraction into the 2000V reflecting drift region. Pulsing into the drift region was done at a frequency of 27 kHz and a pulse width of 1.5 μ s. After leaving the reflector, ions were detected by a multi channel plate detector. The PC computer controlling all the timing and recording the data determined drift times in both the ion mobility and mass portions of the instrument based off a single event recorded at the MCP detector. This was possible due to the fact that the time ions spent in the drift region of the mass spectrometer was negligible compared to the time spent in the ion mobility drift tube. Data acquisition and timing control of the Bradbury-Nielson gate, in the IMS portion of the instrument and TOFMS extractor were achieved through the use of IonWerks³⁵ TOFMS time-to-digital converter and a dual Pentium III workstation running IonWerks 3D acquisition software. Further data processing was completed using Research Systems IDL virtual machine 6.0 software.³⁶

c) Calculations

The standard for reporting IMS data is the reduced mobility (K_o). It standardizes mobility drift times for temperature and pressure. These calculations were done using the following equation:

$$(1) \quad K_o = \frac{L^2}{t_d V} \left[\frac{273}{T} \right] \left[\frac{P}{760} \right]$$

Where L is the length of the drift region (18 cm), t_d is the experimentally determined drift time of the ion (s), V is the voltage drop across the IMS drift region, T is the temperature in the drift tube (473 or 523 K) and P is atmospheric pressure (689 – 701 torr). K_o then has units of $\text{cm}^2/\text{V}\cdot\text{s}$.

RESULTS AND DISCUSSION

a) Individual Proteins – AP-IMtofMS

Two dimensional AP-IMtofMS data was successfully collected for porcine insulin, bovine insulin, aprotinin, cytochrome c, and lysozyme. Table 1 shows the conditions (concentration, temperature, atmospheric pressure, ESI flow rate, IMS electric field strength and acquisition time) and peak identifications for the aforementioned proteins. Figure 1 represents the 2D composite of mass and mobility data for porcine insulin. Three porcine insulin charge states exhibited baseline resolution in both the mass and mobility spectra. The m/z peak at 1157 Da corresponds to the +5 charge state of porcine insulin with a molecular weight of 5778 Da. This m/z peak had a complimentary drift time of 29.5 ms, which at the experimental conditions yielded a reduced mobility of 0.72. The +4 charge state had an m/z peak at 1446 Da with a corresponding drift time of 31.8 ms ($K_o = 0.67$). Finally, the m/z peak at 1928 Da represented the +3 charge state of porcine insulin and had a corresponding drift time of 40.3 ms ($K_o = 0.54$).

Bovine insulin, being an insulin protein, was similar in structure to porcine insulin but had a molecular weight of 5733 Da. The ability to separate these structurally similar proteins via AP-IMMS was to be investigated in this research. To this end bovine insulin was first sprayed and data collected on it individually. This data is shown in figure 2. Like porcine insulin there were three charge states showing baseline resolutions in both the mass and mobility spectra. Also like porcine insulin they were the same charge states +5, +4 and +3. The m/z peak at 1148 Da corresponded to the +5 charge state while the m/z peak at 1435 Da was the result of the +4 charge state and the m/z peak at 1913 Da corresponded to the +3 charge state. When comparing the m/z peaks for bovine insulin to those for porcine insulin the difference in mass was evident in the m/z peaks. However, when looking at the mobility peaks it was evident that the 1148 (+5) m/z peak had a drift time of 28.8 ms ($K_o = 0.74$), the 1435 Da peak had a corresponding drift time of 31.1 ms ($K_o = 0.69$) and the 1913 Da peak had a drift time of 39.3 ms ($K_o = 0.54$). This showed that while bovine and porcine insulin yielded different m/z values for the same charge states the reduced mobilities were the same or practically the same for each charge state. It would therefore be expected that a mixture of these two proteins would show separation in the mass domain but not in the mobility domain.

Aprotinin was another, slightly larger, protein of interest in this study. Aprotinin has a molecular weight of 6511 Da and as such we might expect a greater number of charge states in the 2D spectrum. This was in fact the case. Figure 3 is the 2D spectrum of the aprotinin protein. There were five peaks present in the mass spectrum and four in the mobility spectrum. The m/z peaks at 538 Da and 1087 Da have the same drift time of 24.4 ms ($K_o = 0.88$). This implies that the

538 Da peak was in fact a fragment of the 1087 Da peak. The 931 Da ($K_o=0.92$) peak represented the +7 charge state while the 1087 Da ($K_o=0.81$) peak was the +6 charge state, the 1304 Da ($K_o = 0.81$) peak was the +5 charge state and the 1628 Da ($K_o = 0.68$) peak matched up with the +4 charge state. This is an example of the usefulness of IMtofMS. In the 2D spectrum it is evident that the four aprotinin charge state peaks roughly fall on a line – a “trend line.” In these experiments protein charge states tend to appear linearly in the 2D spectrum, unless the buildup of charge causes a conformation change in which case a new trend line is established (see Cytochrome c and Lysozyme below). Therefore since the 538 Da ion doesn't fall on the Aprotinin trend line and has the exact same mobility as the 1087 Da ion it can be concluded that the 538 Da ion is a fragment of the 1087 Da ion. There was baseline resolution in the mobility spectrum in all cases except for a slight overlap between the +6 and +7 charge states (23.4 ms and 24.4 ms peaks).

Chicken Cytochrome C was another protein of interest in this study. It exhibited eleven charge states, identified with mass and mobilities in Figure 4. Of these eleven charge states baseline or nearly baseline resolution was achieved for all peaks in both the mobility and mass spectra except for two instances of complete mobility overlap. The m/z peak with a value of 1223 Da, representing the +10 charge state, and the m/z value of 2038, representing the +6 charge state, had corresponding mobility peaks that overlapped one another at a drift time of 36.3 ms ($K_o = 0.59$). Isolation of the +6 charge state peak in the 2D spectrum yielded just its mobility at a drift time of 36.9 ms ($K_o = 0.58$). Isolation of the +10 charge state in the 2D spectrum resulted in a drift time, for only this peak, of 36.3 ms ($K_o = 0.59$). Given that the reduced mobility values were different by only 0.01 and the +10 charge state was a much more intense peak it masked the

+6 charge state mobility peak entirely. The same situation was true for the +9 and +5 charge states. Isolation of the +5 charge state (2446 Da) gave a corresponding IMS drift time of 38.7 ms ($K_0 = 0.56$). Isolation of the +9 charge state (1359 Da) yielded a corresponding drift time of 39.3 ms ($K_0 = 0.55$). Cytochrome c exhibits 3 conformational trend lines. The +15 through +8 charge states fall on one line, a second +8 charge state aligns with the +7 charge state and finally the +6 and +5 charge states fall on a third line.

The final individual protein, for which 2D IMMS data was collected, was Lysozyme, Figure 5. Ten m/z peaks were present in this spectrum, nine of which corresponded to charge states of the lysozyme protein – one charge state is present in two different conformations. In this instance, the reported molecular weight, by sigma-aldrich, was an approximate value. The approximate molecular weight given by sigma-aldrich was 14,300 Da. In this data set there were m/z peaks at 1312, 1443, 1603, 1804, 2061, 2404, 2885, 3606, and approximately 3200 Da. All of these peaks, except the ~3200 Da peak, aligned nicely with a calculated molecular mass of 1.442×10^5 Da. The ~3200 Da peak could not be resolved from the noise and assumed to be some kind of contaminant. While in baseline resolution in the mobility domain wasn't evident in every case all peaks are easily resolved in 2D space. Table 1 shows m/z values, their corresponding charge states and corresponding IMS drift times/reduced mobility values. Two trend lines were evident in the 2D spectrum; +11 through +8 fell on one line while +7 through +4 approximately fell on a second. The 3603 Da m/z value, representing the +4 charge state, had two different mobility values associated with it the larger of the two, 48.7 ms ($K_0 = 0.40$) on the second trend line. The second +4 charge state conformation at 39.1 ms ($K_0 = 0.50$) seemed to be starting a new trend line.

b) Protein Mixtures – AP – IMtofMS

Two mixtures were analyzed using AP-IMtofMS, the first being a mixture of Bovine and Porcine Insulin (100uM) and the second being Bovine Insulin (65uM), Aprotinin (65uM), Cytochrome C (130 uM) and Lysozyme (130 uM). In the Bovine/Porcine insulin mixture the results were pretty much as expected. This spectrum is shown in Figure 6. Separation of the bovine insulin charge states from the porcine insulin charge states was evident in the 1D mass spectrum and in the 2D mass/mobility composite but not in the 1D mobility spectrum. However, the +5 charge state was not present for either protein. The temperature for this experiment was increased to 250°C and it's most probable that the loss of this peak and the corresponding increase in intensity of the +3 charge state was a result of said temperature increase. In addition, the concentration of each individual protein was decreased to 100uM in this experiment which lead to the less intense peaks in the 200uM trials being lost in this one.

The more interesting spectrum, figure 7, was of the second mixture described above. The one dimensional mass spectrum is shown at the top of the figure. Like all mass spectra of protein mixtures via electrospray ionization, this spectrum was quite complicated with many peaks per protein species in the mixture. Baseline resolution was not evident in the mobility spectrum. However, all peaks were resolved in 2D space. Furthermore, analysis of the 2D spectrum using trend lines allowed for rapid identification of Aprotinin (A in Figure 7) and Cytochrome c (B in Figure 7). The second trend line for Lysozyme (C2 in Figure 7) was clearly distinguishable from other species. While at first glance C2 might not appear to be related in anyway to C1 if this trend line could be used to determine the identity of Lysozyme, then it could be possible to

identify the four peaks in C1 as charge states of Lysozyme as well, revealing D2 as the 1148 Da +5 charge state of Insulin.

CONCLUSIONS

This research demonstrated the potential for whole protein analysis using tandem ion mobility-time of flight-mass spectrometry. Furthermore, by focusing solely on the mobility domain in these experiments, the potential for IMS as a stand alone instrument for detecting biomolecules, possibly biotoxins, in aqueous samples such as drinking water, storm water runoff, rivers and lakes was demonstrated. The various charge states of five proteins, detected individually, were shown to be both separable and detectable in the mobility and mass domains. This is the first example of some of these intact proteins being analyzed via an AP-IMtofMS, easily exhibiting 2D baseline resolution as well as baseline resolution in the mass domain and, in most cases, baseline resolution in the mobility domain. Baseline resolution for the various charge states of most proteins in the mobility domain demonstrates the potential for IMS as a stand alone instrument.

This is also the first example of a protein mixture being analyzed using AP-IMtofMS. Baseline resolution was not evident in the one dimensional mobility data. However, baseline resolution was evident in the two dimensional data. The degree to which real environmental water samples would have a mixture of proteins, in this mass range, present within it is, at this point, unknown. The complexity of a real world sample would dictate whether or not IMS as a stand alone monitoring device would be sufficient for a given water sample. At the very least, this data

suggests that IMS could function as a real time monitoring device in the field while the tandem instrument finds its use, when necessary for more complicated samples, back in the lab.

In addition to baseline resolution, the presence of size-to-charge vs. mass-to-charge trend lines is demonstrated for the five individual proteins. The trend line is a compound specific trait that can be used to help identify multiple peaks representing different charge states of the same protein. While trend lines are by no means the perfect answer for interpreting complicated ESI-IMMS spectra, as was evident by the overlap of Lysozyme and Insulin which will only get worse in more complicated applications, they can be a tool in the analysis process. Furthermore trend lines tells us something about the degree to which the protein was folded. More tightly wound proteins will have smaller size to mass ratios and hence a less steep slope on the 2D spectrum. Previous work by Clemmer, Hill, Smith, Guevermont and others has demonstrated that different charge states can take on different conformations, and sometimes one charge state can have several conformations associated with it. It is reasonable to conclude, and supported by this data, that those charge states that have the same conformation will fall on a certain trend line. If the conformation changes and multiple charge states have that same conformation, they will fall on a different trend line. This was evident for the larger proteins Cytochrome C and Lysozyme. Using the evident trend lines as a means of analyzing Cytochrome C, three trend lines, representing three spatial conformations, are readily apparent.

ACKNOWLEDGEMENTS

The authors acknowledge dTech, Seattle, WA for partial support of this work through an STTR grant from the National Science Foundation.

REFERENCES

1. Wittmer, D.; Chen, Y.H.; Luckenbill, B.K.; Hill, H.H. *Anal. Chem.*, **1994**, 66, 2348-2355.
2. Chen, Y.H.; Hill, H.H.; Wittmer, D.P. *International J. Mass Spec. and Ion Proc.* **1996** 154 1-13.
3. Shvartsburg, A.A., Bryyskiewicz, T., Purves, R.W., Tang, K., Guevermont, R., Smith R.D. *J. of Phys. Chem. B.* **2006**, 110(43), 21966-21980.
4. Shvartsburg, A.A., Li, F., Tang, K., Smith, R.D. *Anal. Chem.* **2006**, 78, 3304-3315.
5. Badman, E.R.; Myung, S.; Clemmer, D.E. *J. Am. Soc. Mass Spectrom.* **2005**, 16, 1493-1497.
6. Clemmer, D.E.; Hudgins, R.R.; Jarrold, M.F. *J. Am. Chem. Soc.* **1995**, 117, 10141 – 10142.
7. Clemmer, D.E.; Jarrold, M.F. *J. of Mass Spec.* **1997**, 32, 577-592.
8. Shelimov, K.B.; Clemmer, D.E.; Hudgins, R.R.; Jarrold, M.F. *J. Am. Chem. Soc.* **1997**, 119, 2240-2248.
9. Badman, E.R.; Hoaglund-Hyzer, C.S.; Clemmer, D.E. *Anal. Chem.* **2001**, 73, 6000-6007.
10. Wu, C.; Siems, W.F.; Asbury, G.R.; Hill, H.H. *Anal. Chem.* **1998**, 70, 4929-4938.
11. Thalassions, K., Slade, S.E., Jennings, K.R., Scrivens, J.H., Giles, K., Wildgoose, J., Hoyes, J., Bateman, R.H., Bowers, M.T. *Int. J. of Mass. Spec.* **2004**, 236, 55-63.
12. Baker, E.S., Clowers, B.H., Li, F., Tang, K., Tolamchev, A.V., Prior, D.C., Belov, M.E., Smith, R.D. *J. Am. Soc. Mass. Spec.* **2007**, 18, 1176-1187.
13. Clowers, B.H., Siems, W.F., Hill, H.H., Massick, S.M. *Anal. Chem.* **2006**, 78, 44-51.
14. Hoaglund, C.S.; Valentine, S.J.; Sporleder, C.R.; Reilly, J.P.; Clemmer, D.E. *Anal. Chem.* **1998**, 70, 2236-2242.
15. Purves, R.W.; Guevremont, R. *Anal. Chem.* **1999**, 71, 2346-2357.
16. Purves, R.W.; Barnett, D.A.; Ells, B.; Guevremont, R. *J. Am. Soc. Mass Spectrom.* **2000**, 11, 738-745.
17. Purves, R.W.; Barnett, D.A.; Guevremont, R. *Int. J. of Mass Spec.* **2000**, 197, 163-177.
18. Purves, R.W.; Barnett, D.A.; Ells, B.; Guevremont, R. *J. Am. Soc. Mass Spectrom.* **2001**, 12, 894-901.
19. Badman, E.R.; Myung, S.; Clemmer, D.E. *Anal. Chem.* **2002**, 74, 4889-4894.
20. Badman, E.R.; Hoaglund-Hyzer, C.S.; Clemmer, D.E. *J. Am. Soc. Mass Spectrom.* **2002**, 13, 719-723.
21. Hoaglund-Hyzer, C.S.; Counterman, A.E.; Clemmer, D.E. *Chem. Rev.* **1999**, 99, 3037-3079.
22. Myung, S.; Lee, Y.L.; Moon, M.H.; Taraszka, J.; Sowell, R.; Koeniger, S.; Hilderbrand, A.E.; Valentine, S.J.; Cherbas, L.; Cherbas, P.; Kaufmann, T.C.; Miller, D.F.; Mechref, Y.; Novotny, M.V.; Ewing, M.A.; Sporleder, C.R.; Clemmer, D.E. *Anal. Chem.* **2003**, 75, 5137-5145.
23. Moon, M.H.; Myung, S.; Plasencia, M.; Hilderbrand, A.E.; Clemmer, D.E. *Journal of Proteome Research.* **2003**, 2, 589-597.

24. Guevremont, R.; Barnett, D.A.; Purves, R.W.; Vandermeij, J. *Anal. Chem.* **2000**, 72, 4577-4584.
25. Venne, K.; Bonneil, E.; Eng, K.; Thibault, P. *PharmaGenomics*. **May 2004**, 31-40.
26. Merenbloom, S.I., Koeniger, S.L., Valentine, S.J., Plasencia, M.D., Clemmer, D.E. *Anal. Chem.* **2006**, 78, 2802-2809.
27. Koeniger, S.L., Merenbloom, S.I., Valentine, S.J., Jarrold, M.F., Udseth, H.R., Smith, R.D., Clemmer, D.E. *Anal. Chem.* **2006**, 78, 4161-4174.
28. Merenbloom, S.I., Bohrer, B.C., Koeniger, S.L., Clemmer, D.E. *Anal. Chem.* **2007**, 79, 525-522.
29. Sowell, R.A.; Koeniger, S.L.; Valentine, S.J.; Moon, M.H.; Clemmer, D.E. *J. Am. Soc. Mass Spectrom.* **2004**, 15, 1341-1353.
30. Tang, K.; Li, F.; Shvartsburg, A.A.; Strittmatter, E.F.; Smith, R.D. *Anal. Chem.* **2005**, 77 – 19, 6381 – 6388.
31. Steiner, W.E.; Clowers, B.H.; Matz, L.M.; Siems, W.F.; Hill, H.H., *Anal. Chem.*, **2002**, 74, 4343- 4352.
32. Steiner, W.E.; Clowers, B.H.; Haigh, P.E.; Hill, H.H., *Anal. Chem.*, **2003**, 75, 6068-6076.
33. Steiner W.E.; Clowers B.H.; Fuhrer K.; Gonin M.; Matz L.M.; Siems W.F.; Schultz A.J.; Hill H.H., *Rapid Comm. Mass Spectrom*, **2001**, 15, 2221.
34. Matz, L.M.; Steiner, W.E.; Clowers, B.H.; Hill, H.H. *International J. Mass Spec.* **2002**, 213, 191-202.
35. Ionwerks 3-D, *Ionwerks Inc*, Houston TX, **2004**.
36. Transform V3.4, *Fortner Software LLC*, Serling VA, **1998**. Research Systems IDL virtual machine 6.0, *Research Systems Inc.*, Boulder CO, **2004**.

CAPTIONS

Table 1 – AP-IMtofMS of Proteins

Figure 1: The 2D composite of mass and mobility data for porcine insulin showing baseline resolution of three porcine insulin charge states in both the mass and mobility domains. m/z values, charges states, drift times and reduced mobility values are identified for each peak. The sample was 200uM and collected at 200°C, 701 torr, 5uL/min, 441.1 V/cm for 30 minutes.

Figure 2 - The 2D composite of mass and mobility data for a 200uM sample of bovine insulin at 200°C, 689 torr, 5uL/min and 441.1 V/cm for 30 minutes. The spectrum shows baseline resolution of three insulin charge states in both the mass and mobility domains. Charge state, m/z value, drift time and reduced mobility are identified for all peaks.

Figure 3 - 2D composite spectrum of 200uM aprotinin collected at 200°C, 695 torr, 5uL/min and 441.1 V/cm for 30 minutes. The spectrum shows 5 peaks. One is identified as a fragment peak while the other four are identified as aprotinin charge states. Charge state (or designation as fragment), m/z value, drift time and reduced mobility are identified for all peaks present in the spectrum.

Figure 4 – 2D spectrum of mass and mobility for a 200uM sample of Cytochrome C taken at 200°C, 695 torr, 5uL/min and 441.1 V/cm for 60 minutes. The spectrum shows twelve peaks, all of which are identified as Cytochrome C charge states. One charge state (+8) is shown to have two conformations – hence two drift times.

Figure 5 – 2D spectrum of mass and mobility for 100 uM sample of Lysozyme collected at 250°C, 696 torr, 5uL/min and 441.1V/cm for 60 minutes. Ten features are evident: eight are Lysozyme charge states – one of which has two conformations drifting at different drift times, one feature is unidentified.

Figure 6 – 2D mass vs. mobility spectrum for a mixture of porcine and bovine insulin, both at 100uM concentration. Experimental conditions were 250°C, 698 torr, 5 uL/min and 441.1 V/cm for 30 minutes. Two mobilities are present representing 2 charge states. In the mass domain the bovine insulin peak is distinguishable from the porcine insulin peak with the same charge state, not so in the mobility domain.

Figure 7 – 2D spectrum, mass vs. mobility for a mixture of 130 uM Cytochrome C, 130 uM Lysozyme, 65 uM Aprotinin and 65uM Insulin at 200°C, 698 torr, 5 uL/min and 441.1 V/cm for 150 minutes. Proteins are shown to exhibit mass to mobility ratios that fall on compound specific trend lines. Trend lines can be used to quickly identify charge state peaks belonging to one protein or another.

| Table 1 – AP-IMtofMS of Proteins | | | | | |
|---|--|-------------|---------------------|--|--|
| Protein | Conditions | m/z | Charge State | Drift time (ms) - K₀ | |
| Porcine Insulin | 200 μM 200°C 701 torr 5 μL/min 406.7 V/cm 30 min | 1157 | +5 | 29.5 - 0.72 | |
| | | 1446 | +4 | 31.8 - 0.67 | |
| | | 1928 | +3 | 40.3 - 0.54 | |
| Bovine Insulin | 200 μM 200°C 689 torr 5 μL/min 406.7 V/cm 30 min | 1148 | +5 | 28.8 - 0.73 | |
| | | 1435 | +4 | 31.1 - 0.69 | |
| | | 1913 | +3 | 39.3 - 0.54 | |
| Aprotinin | 200 μM 200°C 695 torr 5 μL/min 406.7 V/cm 30 min | 538 | +6 Frag. | 24.4 - 0.88 | |
| | | 931 | +7 | 23.4 - 0.92 | |
| | | 1087 | +6 | 24.4 - 0.88 | |
| | | 1304 | +5 | 26.6 - 0.81 | |
| | | 1628 | +4 | 31.9 - 0.67 | |
| Cytochrome C | 200 μM 200°C 695 torr 5 μL/min 406.7 V/cm 60 min | 815 | +15 | 29.0 - 0.74 | |
| | | 874 | +14 | 30.1 - 0.72 | |
| | | 941 | +13 | 31.1 - 0.69 | |
| | | 1020 | +12 | 32.5 - 0.66 | |
| | | 1113 | +11 | 34.2 - 0.63 | |
| | | 1223 | +10 | 36.3 - 0.59 | |
| | | 1359 | +9 | 39.4 - 0.55 | |
| | | 1529 | +8 | 37.8 - 0.57 | |
| | | 1529 | +8 | 42.7 - 0.50 | |
| | | 1748 | +7 | 40.3 - 0.53 | |
| | | 2038 | +6 | 36.3 - 0.59 | |
| 2446 | +5 | 39.4 - 0.55 | | | |
| Lysozyme | 100 μM 250°C 696 torr 5 μL/min 406.7 V/cm 60 min | 1311 | +11 | 29.9 - 0.65 | |
| | | 1443 | +10 | 31.0 - 0.63 | |
| | | 1603 | +9 | 32.4 - 0.60 | |
| | | 1803 | +8 | 34.3 - 0.57 | |
| | | 2063 | +7 | 31.8 - 0.61 | |
| | | 2403 | +6 | 33.9 - 0.58 | |
| | | 2886 | +5 | 39.6 - 0.49 | |
| | | ~3200 | ? | | |
| | | 3603 | +4 | 39.1 - 0.50 | |
| | | 3603 | +4 | 48.7 - 0.40 | |
| Bovine/Porcine Insulin Mixture | 100 μM 250°C 698 torr 5 μL/min 406.7 V/cm 30 min | | | | |
| Protein Mixture | Cyt. C/Lys. – 130uM Apr./Ins. – 130 uM 200°C 698 torr 5ul/min 406.7 V/cm 150 min | | | | |

Figure 1: The 2D composite of mass and mobility data for porcine insulin showing baseline resolution of three porcine insulin charge states in both the mass and mobility domains. m/z values, charges states, drift times and reduced mobility values are identified for each peak. The sample was 200uM and collected at 200°C, 701 torr, 5uL/min, 441.1 V/cm for 30 minutes.

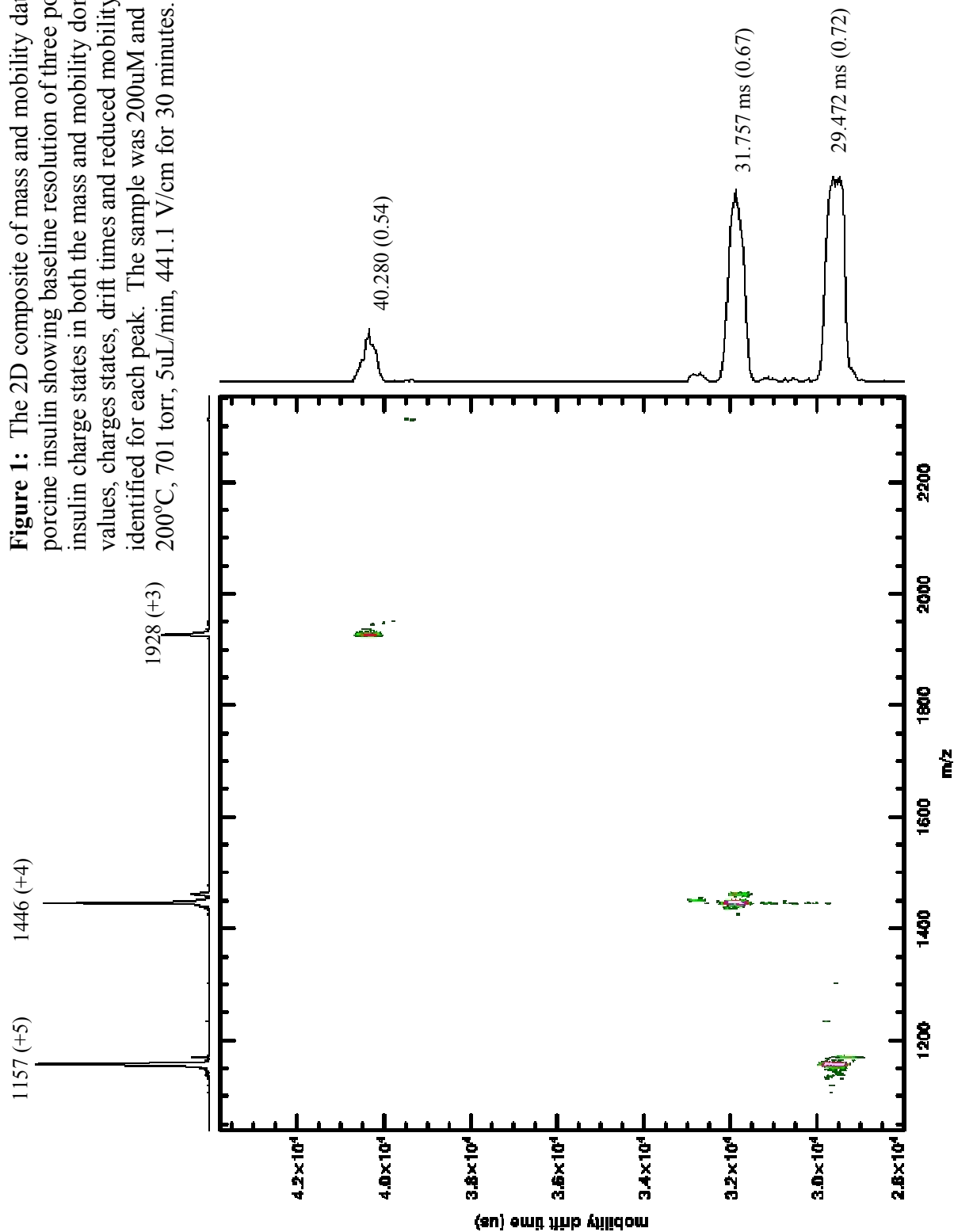


Figure 2 - The 2D composite of mass and mobility data for a 200uM sample of bovine insulin at 200°C, 689 torr, 5uL/min and 441.1 V/cm for 30 minutes. The spectrum shows baseline resolution of three insulin charge states in both the mass and mobility domains. Charge state, m/z value, drift time and reduced mobility are identified for all peaks.

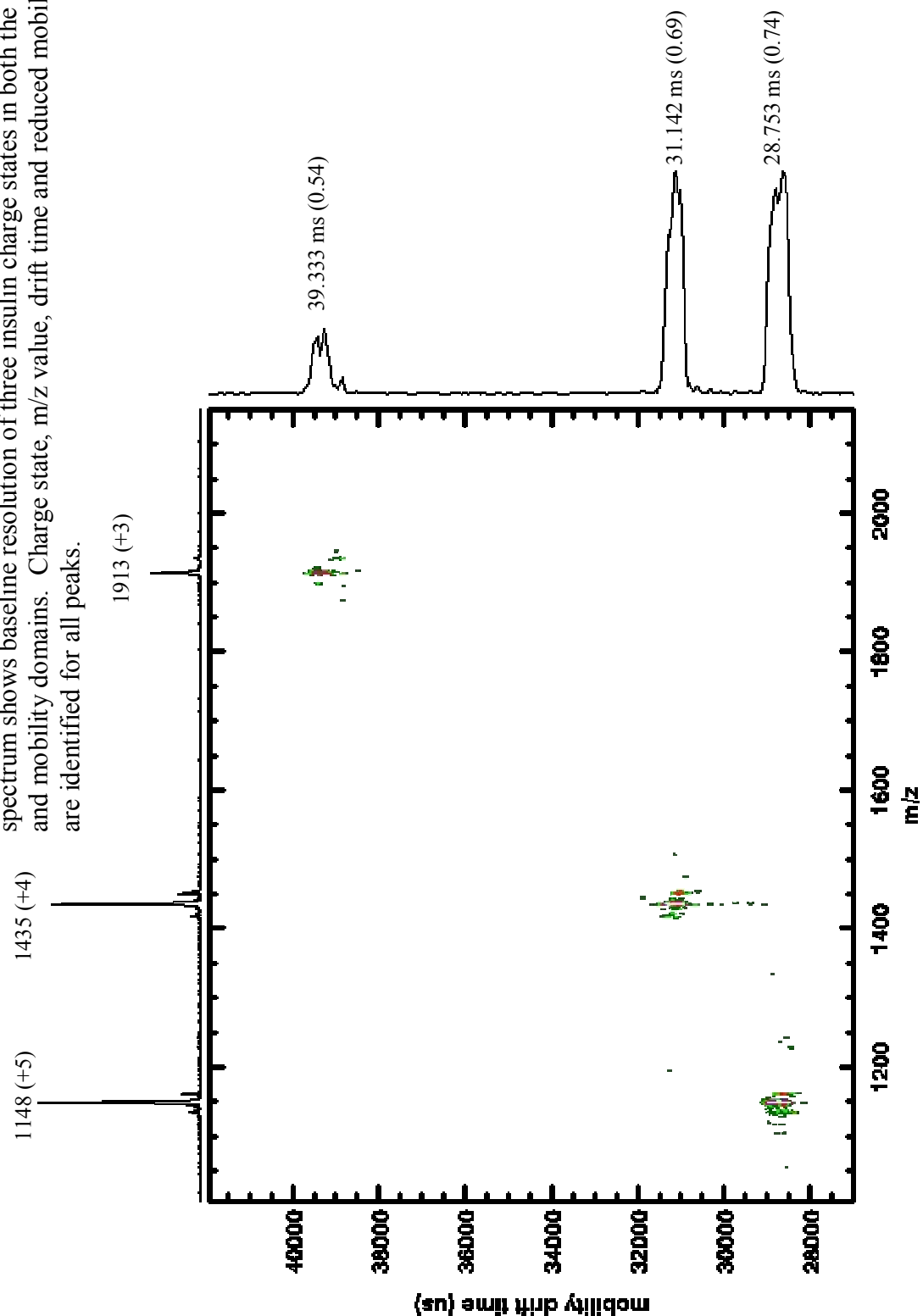


Figure 3 - 2D composite spectrum of 200uM aprotinin collected at 200°C, 695 torr, 5uL/min and 441.1 V/cm for 30 minutes. The spectrum shows 5 peaks. One is identified as a fragment peak while the other four are identified as aprotinin charge states. Charge state (or designation as fragment), m/z value, drift time and reduced mobility are identified for all peaks present in the spectrum.

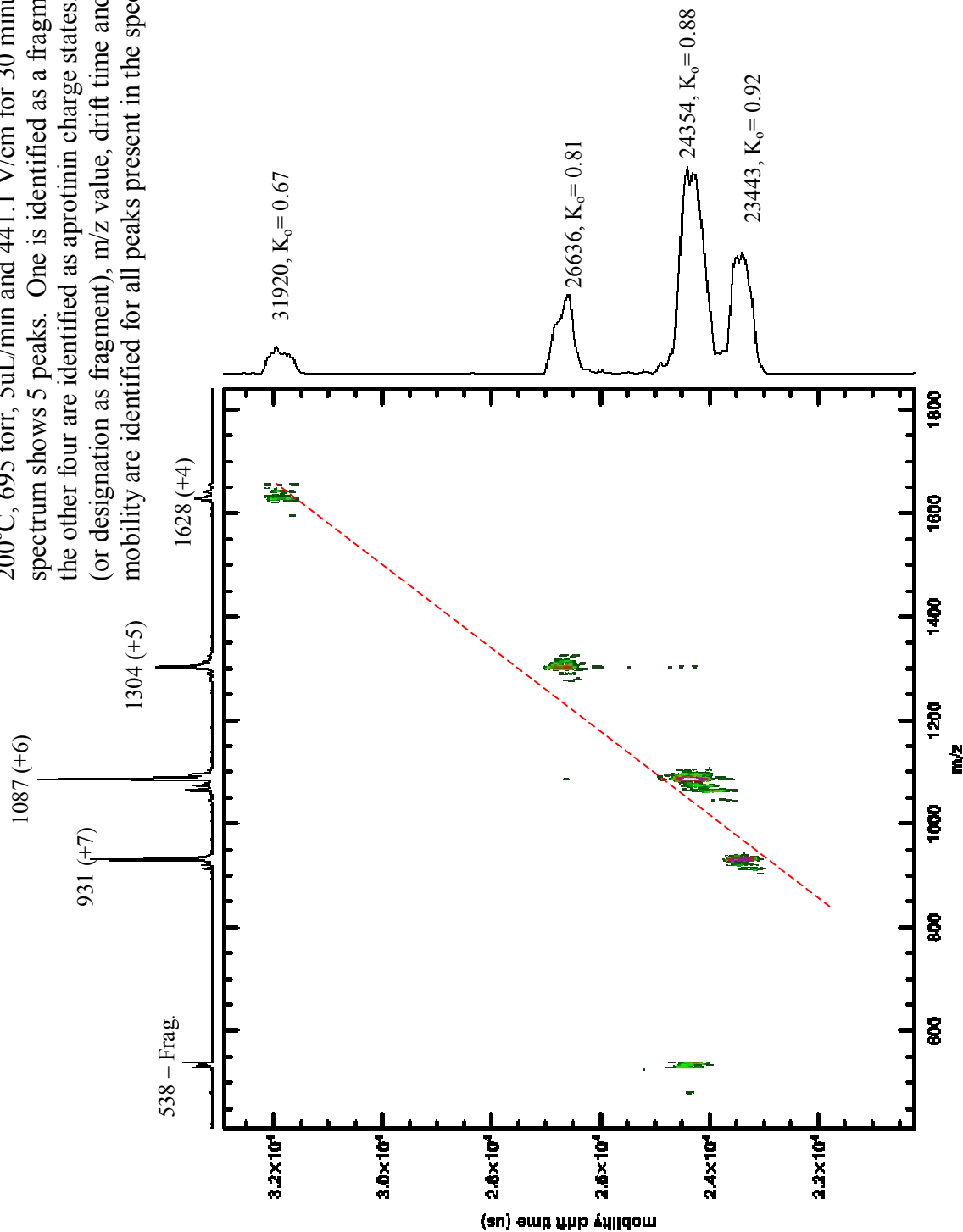


Figure 4 – 2D spectrum of mass and mobility for a 200uM sample of Cytochrome C taken at 200°C, 695 torr, 5uL/min and 441.1 V/cm for 60 minutes. The spectrum shows twelve peaks, all of which are identified as Cytochrome C charge states. One charge state (+8) is shown to have two conformations – hence two drift times.

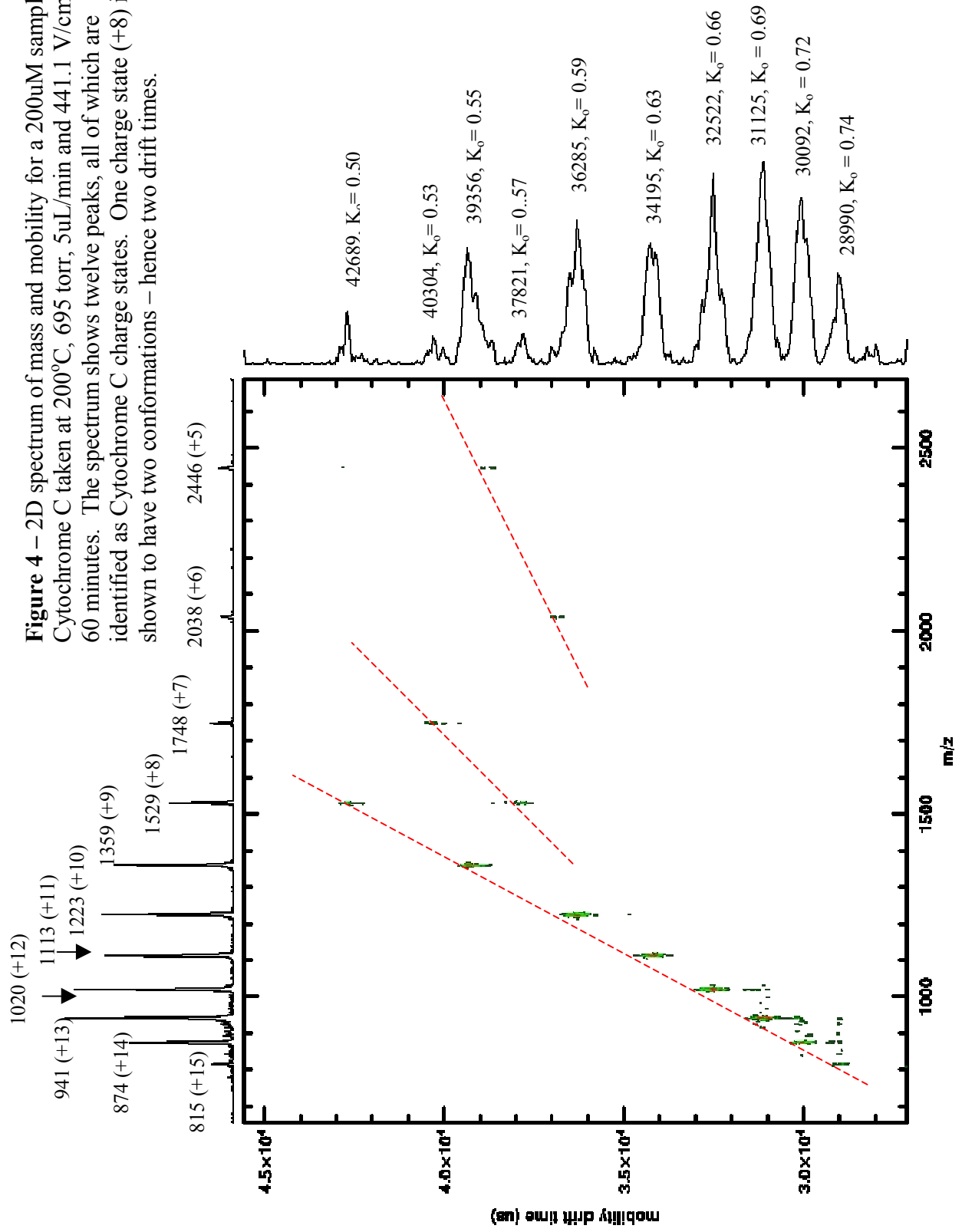
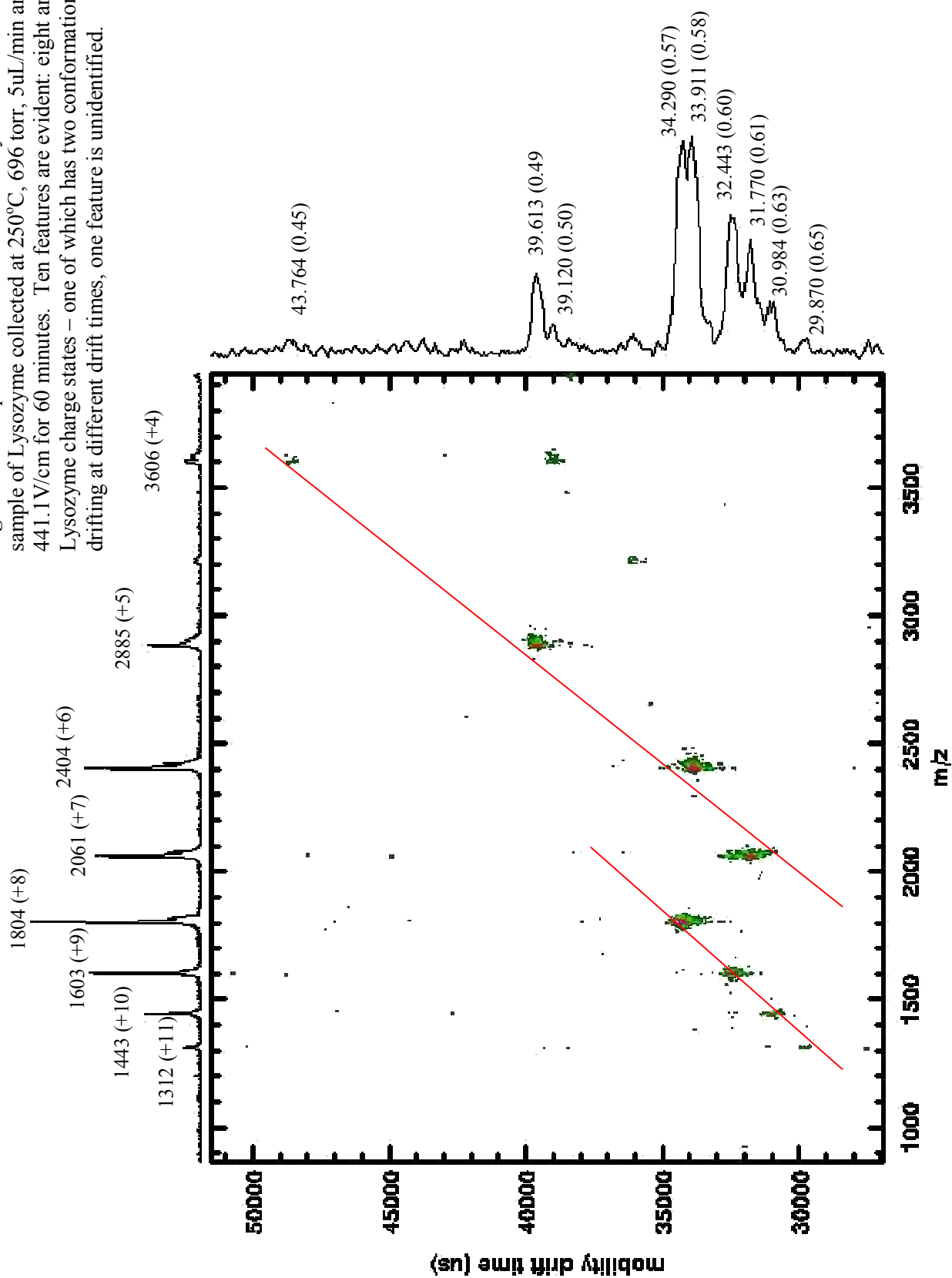


Figure 5 – 2D spectrum of mass and mobility for 100 uM sample of Lysozyme collected at 250°C, 696 torr, 5uL/min and 441.1V/cm for 60 minutes. Ten features are evident: eight are Lysozyme charge states – one of which has two conformations drifting at different drift times, one feature is unidentified.



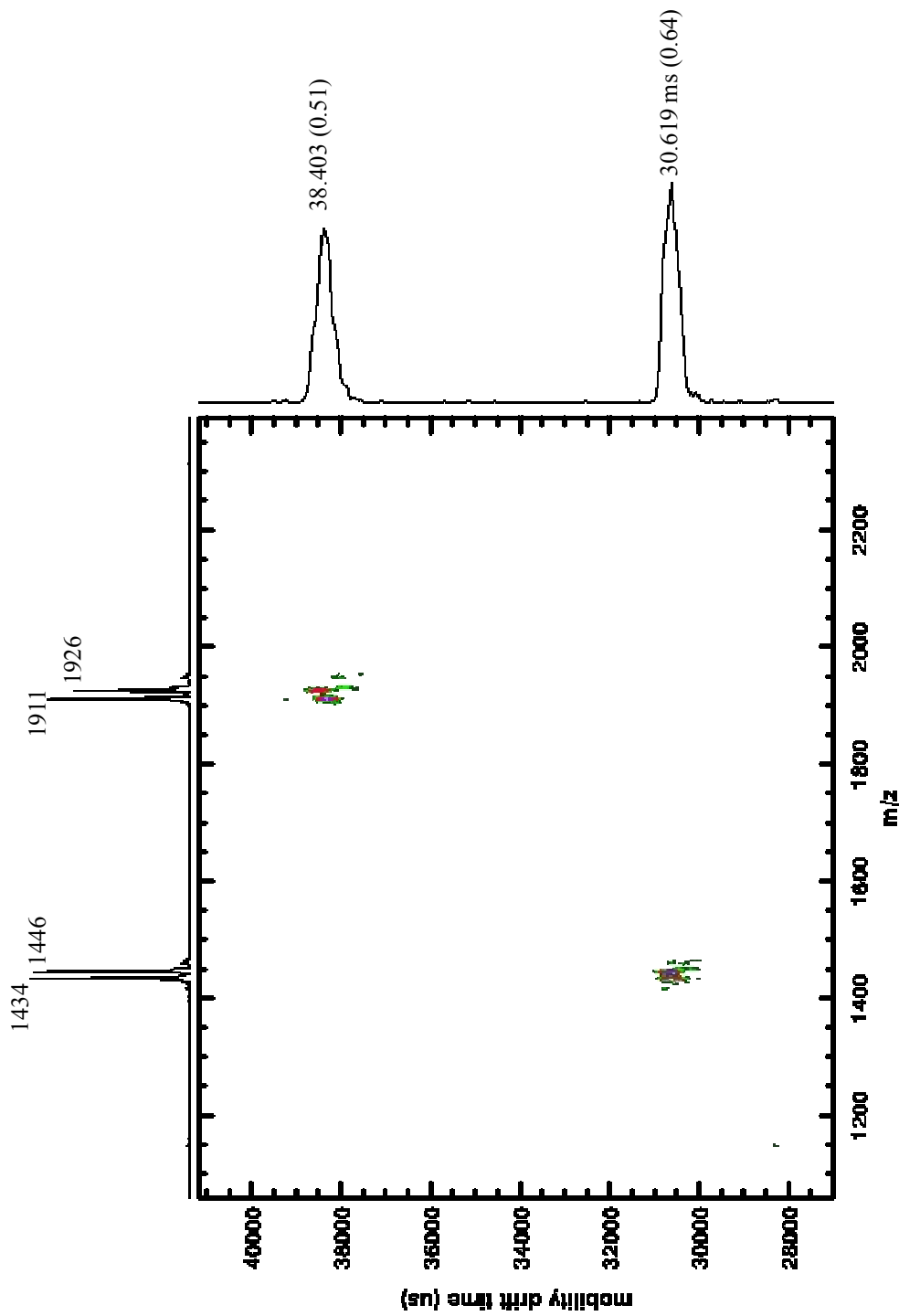


Figure 6 – 2D mass vs. mobility spectrum for a mixture of porcine and bovine insulin, both at 100uM concentration. Experimental conditions were 250°C, 698 torr, 5 uL/min and 441.1 V/cm for 30 minutes. Two mobilities are present representing 2 charge states. In the mass domain the bovine insulin peak is distinguishable from the porcine insulin peak with the same charge state, not so in the mobility domain.

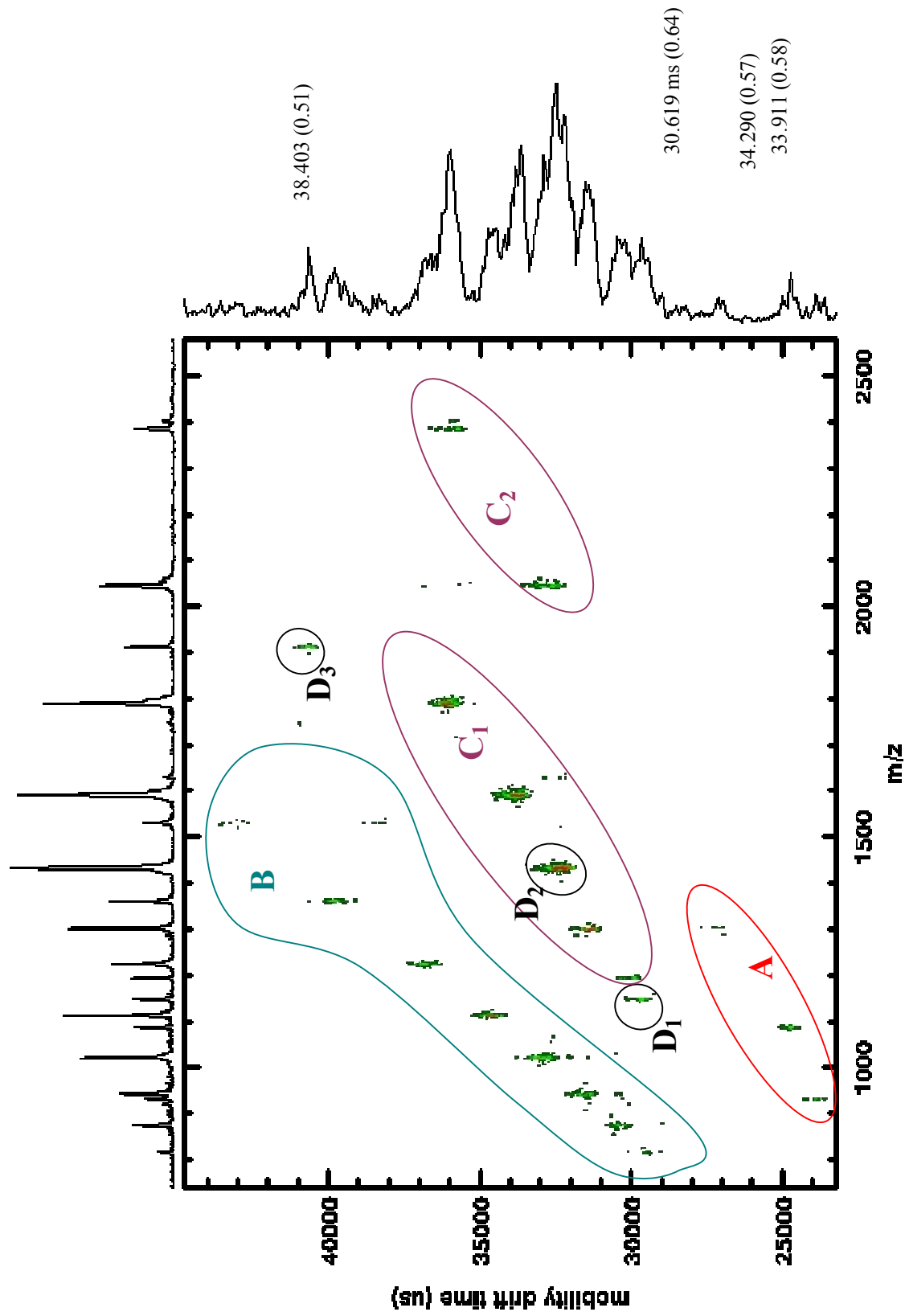


Figure 7 – 2D spectrum, mass vs. mobility for a mixture of 130 uM Cytochrome C, 130 uM Lysozyme, 65 uM Aprotinin and 65uM Insulin at 200°C, 698 torr, 5 uL/min and 441.1 V/cm for 150 minutes. Proteins are shown to exhibit mass to mobility ratios that fall on compound specific trend lines. Trend lines can be used to quickly identify charge state peaks belonging to one protein or another.

CHAPTER 4

CONCLUSION

This work looked at novel applications of ion mobility spectrometry, specifically, its application to real time monitoring of inorganic environmental contaminants in aqueous media and the detection and separation of intact proteins in aqueous media. While these experiments were all conducted on an ESI-IM(tof)MS instrument, it was suggested, by focusing solely on the mobility domain of the tandem experiments, that a stand alone IMS instrument could be used for real time monitoring in the field while the tandem instrument finds its usefulness back in the lab. Mobility peaks can be mass identified in the lab, K_0 values determined and then these can be used for analysis in the field.

Specific inorganic analytes of interest were arsenic compounds, nitrate, nitrite, chloride, sulfate and phosphate anions. While some of these had been detected individually, on a stand alone IMS instrument, in previous work, mixtures had not been successfully analyzed. Likewise, while K_0 values have been assigned to some of the analytes of interest in these stand alone IMS experiments none of the peaks had been mass identified. This work either confirmed the identity and K_0 values of previous work or new peaks were identified and K_0 values added to the scientific literature. Furthermore, a mixture of all the above analytes was successfully separated and detected via the tandem instrument. In the two dimensional mass/mobility spectrum all twenty-one peaks exhibit baseline resolution. Some of these peaks can be identified as fragments resulting from the pressure differential in the interface between the atmospheric pressure IMS and the low vacuum mass spectrometer. As such, they show one mobility peak.

One important result of this experiment, which demonstrates the potential for IMS to function independently in the field, is the baseline resolution of all peaks evident in the mobility domain. Determination of reduced mobility values and mass identification of peaks of interest, as performed in this experiment, is essential for the future application of stand alone IMS in the field. Reproducing this experiment with anionic inorganic contaminants of environmental import, with the degree of baseline resolution presented here, in a stand alone instrument, which has been previously demonstrated with other analytes, would confirm an excellent possibility for the real time monitoring of inorganic contaminants, at fairly low detection limits in the low ppm range, using ESI-IMS.

Protein analyses conducted in this work had two objectives. One objective was to show the potential for a stand alone IMS to detect intact proteins from aqueous media in real time. The second objective was to demonstrate the usefulness of ion mobility as the sole separations technique in the analysis of protein mixtures. Successfully separating and identifying proteins is of great interest in the field of proteomics and this work is intended to show the potential for IMtofMS within the field. While IMMS systems have been employed to similar ends previously all examples included an LC separations step and were low pressure IMS separations. This work is intended to show the potential atmospheric pressure IMS has without the LC step.

Individual proteins analyzed in this work were Insulin, Aprotinin, Lysozyme and Cytochrome C. All proteins exhibited multiple charge states easily showing baseline resolution in the three dimensional mass, mobility intensity spectra. Likewise baseline resolution was evident in both the mass and mobility domains – with the exception of two Lysozyme peaks in the mobility

domain. If a stand alone instrument exhibited the same resolution and sensitivity as this one it could easily detect and separate individual proteins. However, as is evident in this work, mixtures of intact proteins, all with their respective charge states, present complicated spectra with many peaks and baseline resolution in the mobility domain was simply not achievable. Baseline resolution was achievable in the mass domain but identifying the parent protein becomes a challenge as one needs to identify which of the many peaks belong to which protein. Consequently the usefulness of IMS as a stand alone instrument for detection of biomolecules, possibly biotoxins, in the environment would depend on the complexity of the real world samples. Samples IMS alone could not resolve in the field could be brought back to the lab for more detailed IMtofMS work.

The two dimensional mass/mobility spectra produced in this experiment exhibited mass vs. mobility peaks that fell on certain trend lines. These trend lines are indicative of the folding of the protein and since the nature of protein folding is protein specific this trend line can be used to isolate which of the many peaks in a complicated spectrum belong to which proteins. The process is not perfect since it's been shown that different charges states can exhibit different three dimensional folding patterns. The result of this differential folding based on charge is that one protein can have mass vs. mobility peaks falling on multiple trend lines, making the analysis more difficult. In addition, trend lines of different proteins can and do overlap. Therefore, while the analysis isn't perfect this work shows the potential for much simplified protein analysis over a stand alone mass spectrometer. When trend lines are found within the 2D spectrum those peaks falling on the line should be assumed to be the multiple charge states of one protein. From these peaks the mass of the protein can be determined. If there is a large degree of disagreement

between the calculated protein mass as determined from multiple peaks then there is probably overlap of trend lines and deeper analysis is required. The mixture used in this experiment; Insulin, Aprotinin, Lysozyme and Cytochrome C showed that two of the four proteins fell on trend lines that were completely separate from the trend lines of the other proteins. Two of the proteins had overlapping trend lines. While distinguishing peaks belonging to one protein from those belonging to another in the overlapping region would require more work, the process is much simplified from a stand alone MS experiment in that masses of two of the four proteins in the mixture are easily and almost immediately identified narrowing the field for the remaining peaks.

Further work on this project, specific to the detection and inorganic anionic species, should include optimizing and using a stand alone instrument for real time analysis of drinking water supplies, storm water runoff, etc... In order to facilitate this work further IMMS work should be completed so as to analyze and identify K_o values for analytes of environmental interest. With these new K_o values along with previously determined ones and fabrication of a portable field instrument this real time analysis could be accomplished.

With regards to work with proteins, this project should include changing and/or better optimizing the atmospheric pressure interface. Low ion transmission resulted in fairly long data acquisition times. The protein mixture data took 2.5 hours to collect. While comparable or better than similar LC separations the potential for much faster data acquisition times exists in this experiment. Transmitting large ions through this interface required reduction of the ion current by roughly three-fourths. An interface that allowed for transmission of large analytes while

maintaining ion counts should significantly reduce data acquisition time – possibly as short as half an hour for this very same sample – based on similar experiments with smaller analytes. Comparable to most other protein separation techniques this is would be a very good acquisition time.